Interstellar magnetic fields

Martin Houde
The University *of* Western Ontario

1 Interstellar magnetic fields

In this lecture I will cover some of the physical processes that are central to studies of magnetic fields in the interstellar medium (ISM), and the related techniques developed and used for their characterization. The field of research centred on this topic have significantly evolved in recent years and, as a consequence, not all techniques can be covered in a single lecture; we will therefore focus on a few from the more commonly used.

1.1 The Stokes parameters

Most (but not all) studies of interstellar magnetic fields involve the measurements of polarization either in spectral lines or in continua (e.g., from dust or charged particles). It will therefore be beneficial to first consider how polarization states are modelled before investigating the different physical processes responsible for polarized signals and the techniques used in subsequent analyses.

We consider the propagation of electromagnetic plane waves and define two waves propagating in the same direction $\mathbf{n}$ with

$$\mathbf{E}_1 = \mathbf{e}_1 E_1 e^{i(\mathbf{k}\cdot\mathbf{x}-\omega t)} \tag{1.1}$$

$$\mathbf{E}_2 = \mathbf{e}_2 E_2 e^{i(\mathbf{k}\cdot\mathbf{x}-\omega t)} \tag{1.2}$$

$$\mathbf{B}_j = \sqrt{\mu\epsilon}\,\mathbf{n} \times \mathbf{E}_j, \tag{1.3}$$

Outline

- Polarization and Stokes parameters
- Polarization from spectral lines
    - Zeeman effect
    - Goldreich-Kylafis effect
- Polarization from dust
    - Differential absorption
    - Emission
- Polarization in the radio
    - Synchrotron
    - Faraday rotation, depolarization and B field strength
- Davis-Chandrasekhar-Fermi equation
- Dispersion analysis

Stokes parameters

$$\mathbf{E}(\mathbf{x},t) = (\mathbf{e}_1 E_1 + \mathbf{e}_2 E_2)\, e^{i(\mathbf{k}\cdot\mathbf{x}-\omega t)}.$$

$$E_j = a_j e^{i\delta_j}$$

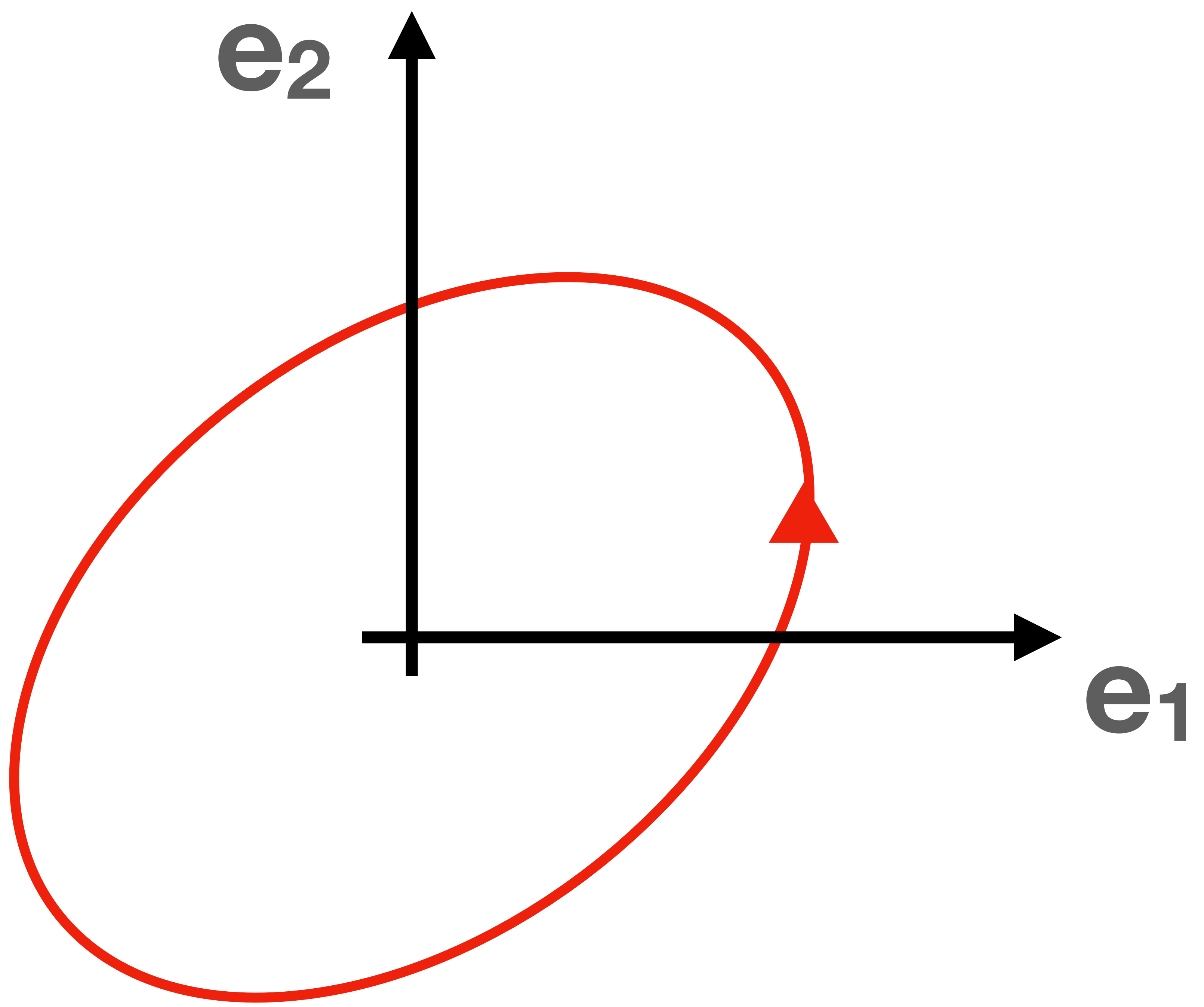

Stokes parameters

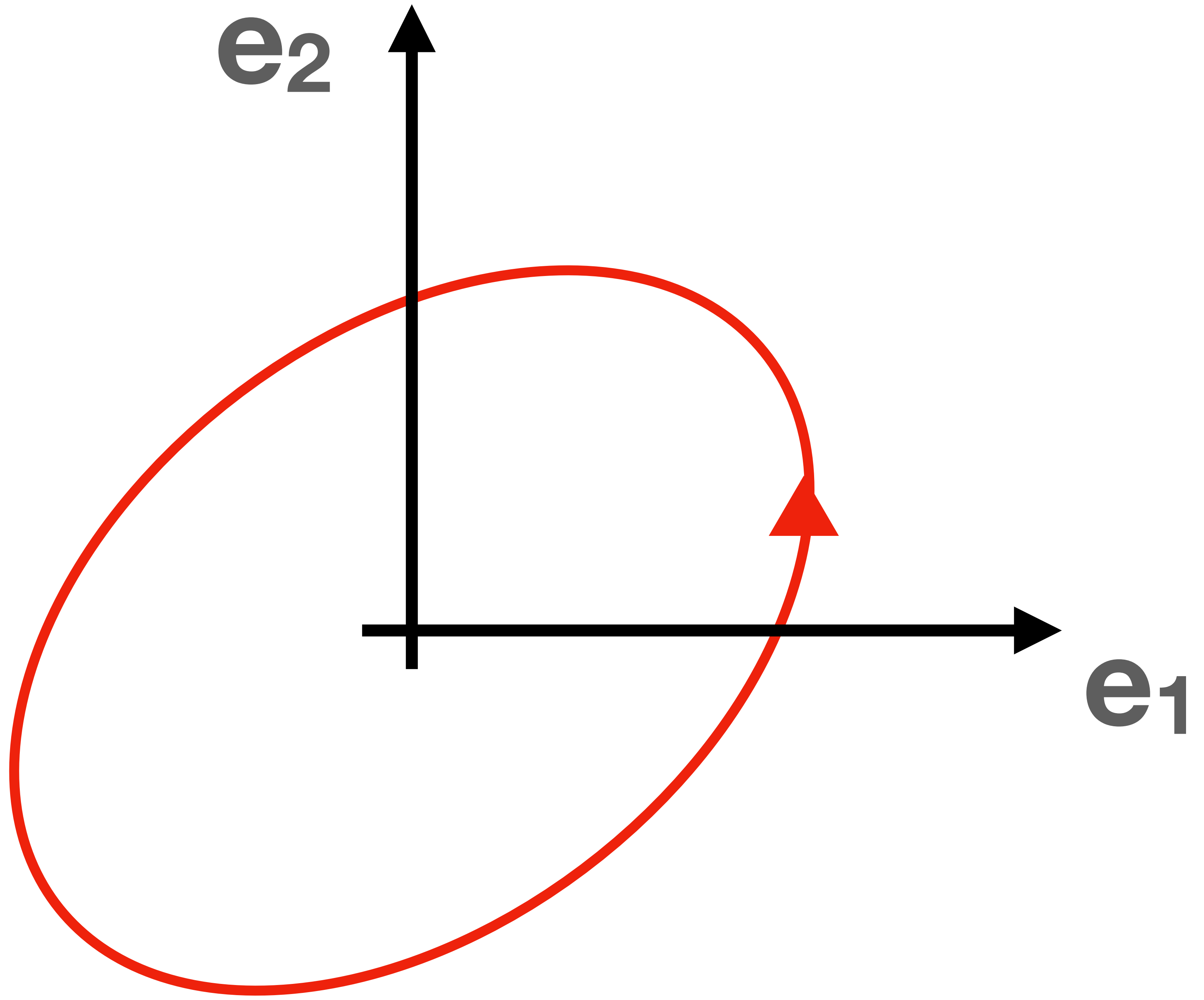

$$\mathbf{E}(\mathbf{x},t) = (\mathbf{e}_1 E_1 + \mathbf{e}_2 E_2)\, e^{i(\mathbf{k}\cdot\mathbf{x}-\omega t)}.$$

$$E_j = a_j e^{i\delta_j}$$

$$\begin{aligned} I &= |\mathbf{e}_1 \cdot \mathbf{E}|^2 + |\mathbf{e}_2 \cdot \mathbf{E}|^2 \\ &= a_1^2 + a_2^2 \qquad (1.17) \\ Q &= |\mathbf{e}_1 \cdot \mathbf{E}|^2 - |\mathbf{e}_2 \cdot \mathbf{E}|^2 \\ &= a_2^2 - a_1^2 \qquad (1.18) \\ U &= 2\,\mathrm{Re}\left[(\mathbf{e}_1 \cdot \mathbf{E})^* (\mathbf{e}_2 \cdot \mathbf{E})\right] \\ &= 2\, a_1 a_2 \cos(\delta_2 - \delta_1) \qquad (1.19) \\ V &= 2\,\mathrm{Im}\left[(\mathbf{e}_1 \cdot \mathbf{E})^* (\mathbf{e}_2 \cdot \mathbf{E})\right] \\ &= 2\, a_1 a_2 \sin(\delta_2 - \delta_1) \qquad (1.20) \end{aligned}$$

Stokes parameters

$$\mathbf{E}\left(\mathbf{x},t\right)=\left(\mathbf{e}_{+}E_{+}+\mathbf{e}_{-}E_{-}\right)e^{i(\mathbf{k}\cdot\mathbf{x}-\omega t)}$$

$$\mathbf{e}_{\pm}=\frac{1}{\sqrt{2}}\left(\mathbf{e}_{1}\pm i\mathbf{e}_{2}\right)$$

$$\begin{aligned}E_{+}&=\frac{1}{\sqrt{2}}\left(E_{1}-iE_{2}\right)\\E_{-}&=\frac{1}{\sqrt{2}}\left(E_{1}+iE_{2}\right)\end{aligned}$$

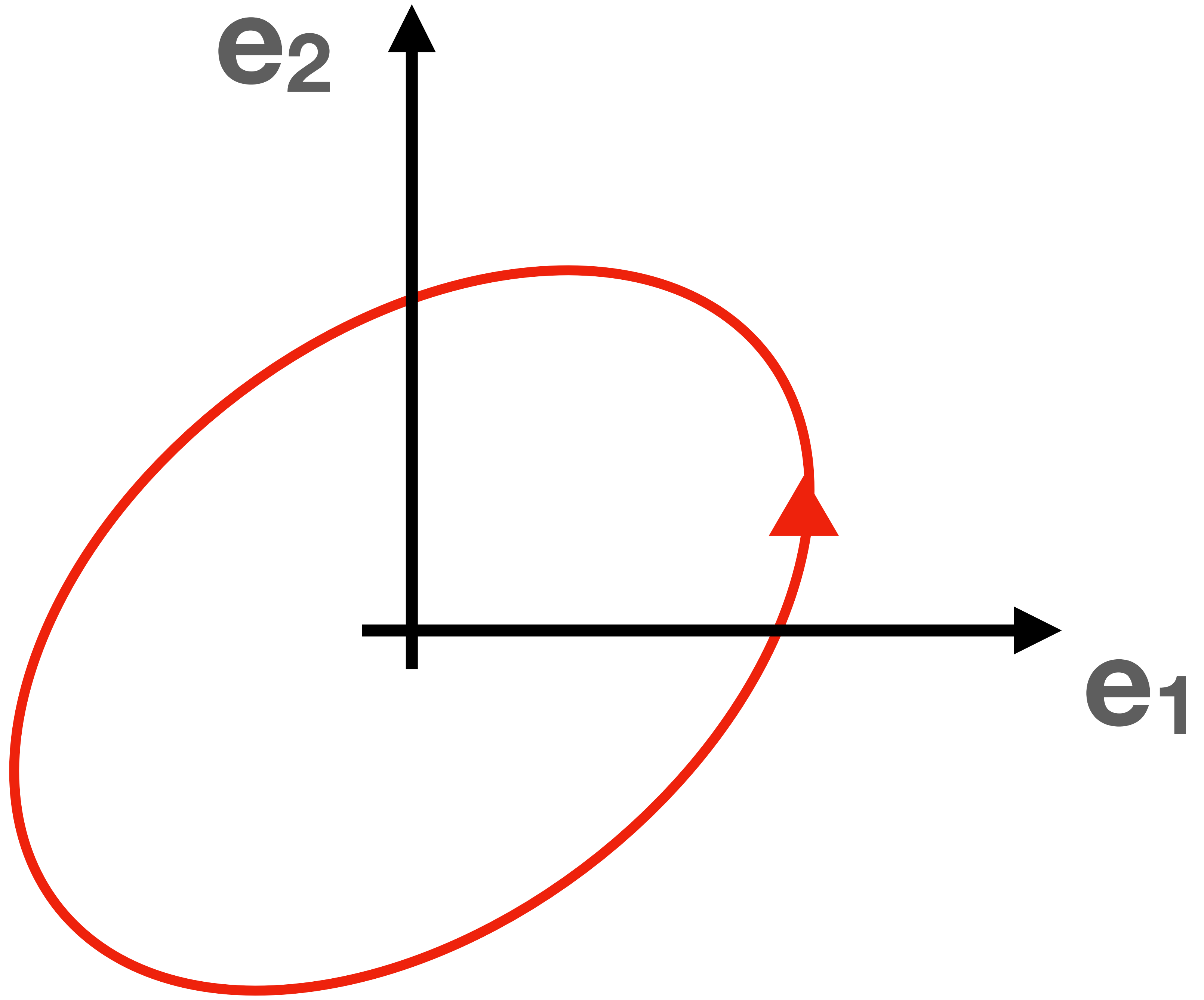

Stokes parameters

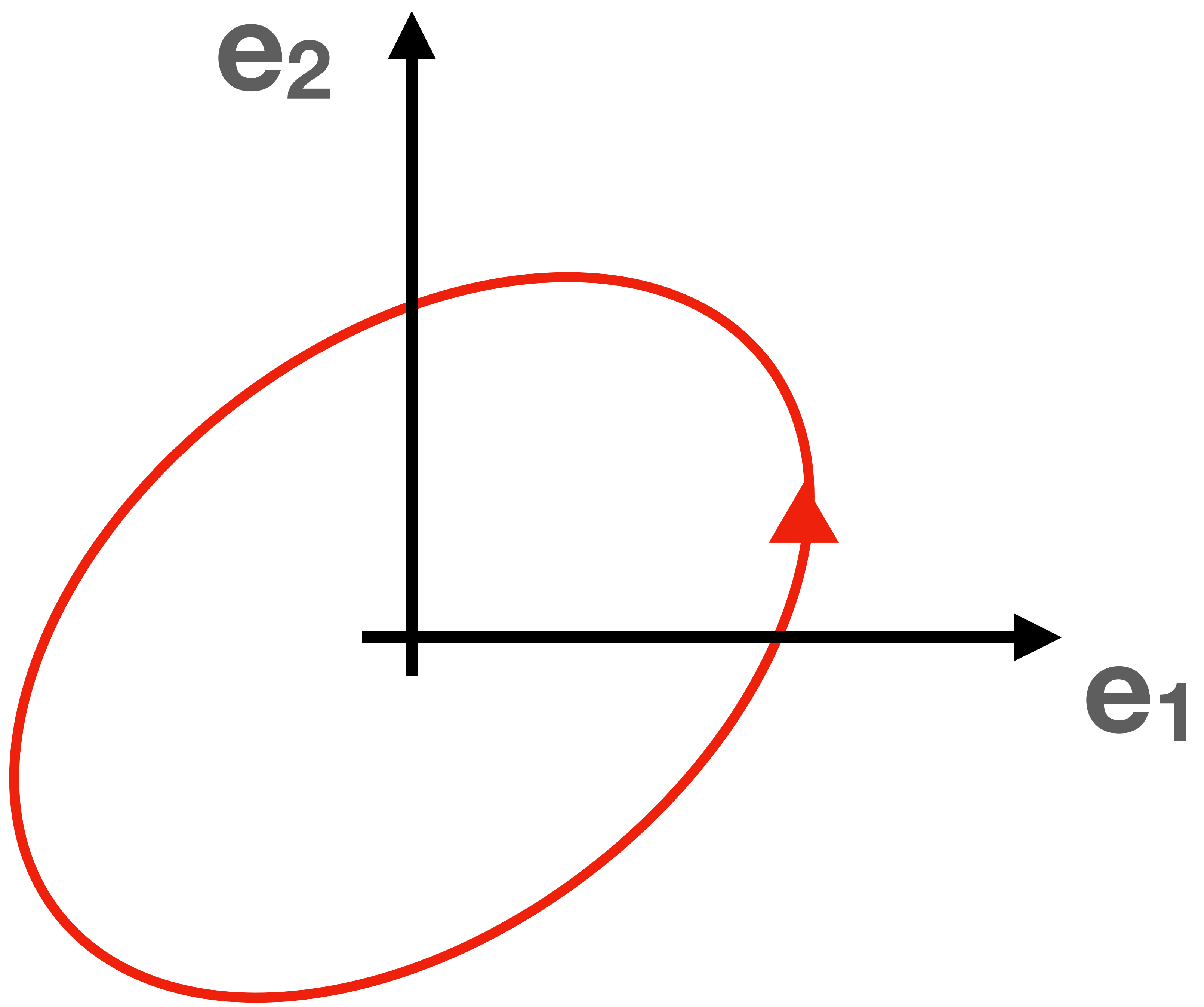

$$\mathbf{E}\left(\mathbf{x},t\right) = \left(\mathbf{e}_+ E_+ + \mathbf{e}_- E_-\right) e^{i(\mathbf{k}\cdot\mathbf{x}-\omega t)}$$

$$\mathbf{e}_\pm = \frac{1}{\sqrt{2}}\left(\mathbf{e}_1 \pm i\mathbf{e}_2\right)$$

$$\begin{aligned} E_+ &= \frac{1}{\sqrt{2}}\left(E_1 - iE_2\right) \\ E_- &= \frac{1}{\sqrt{2}}\left(E_1 + iE_2\right) \end{aligned}$$

$$\begin{aligned} I &= \left|\mathbf{e}_+^* \cdot \mathbf{E}\right|^2 + \left|\mathbf{e}_-^* \cdot \mathbf{E}\right|^2 \\ &= a_+^2 + a_-^2 && (1.21) \\ Q &= 2\,\mathrm{Re}\left[\left(\mathbf{e}_+^* \cdot \mathbf{E}\right)^* \left(\mathbf{e}_-^* \cdot \mathbf{E}\right)\right] \\ &= 2\,a_+ a_- \cos\left(\delta_- - \delta_+\right) && (1.22) \\ U &= 2\,\mathrm{Im}\left[\left(\mathbf{e}_+^* \cdot \mathbf{E}\right)^* \left(\mathbf{e}_-^* \cdot \mathbf{E}\right)\right] \\ &= 2\,a_+ a_- \sin\left(\delta_- - \delta_+\right) && (1.23) \\ V &= \left|\mathbf{e}_+^* \cdot \mathbf{E}\right|^2 - \left|\mathbf{e}_-^* \cdot \mathbf{E}\right|^2 \\ &= a_+^2 - a_-^2 && (1.24) \end{aligned}$$

Stokes parameters

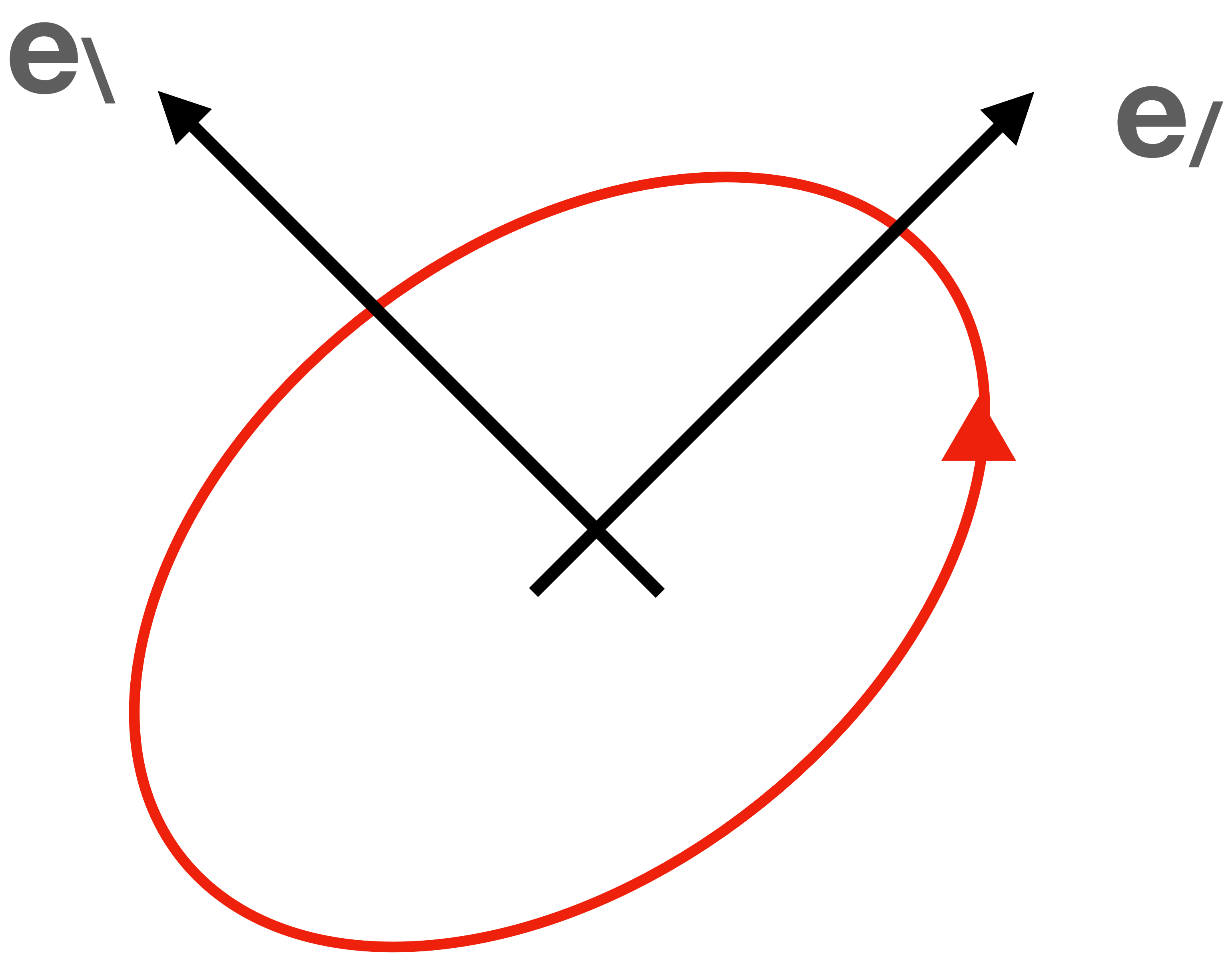

$$\mathbf{e}_/ = \frac{1}{\sqrt{2}}(\mathbf{e}_1 + \mathbf{e}_2)$$
$$\mathbf{e}_\backslash = \frac{1}{\sqrt{2}}(\mathbf{e}_1 - \mathbf{e}_2)$$

Stokes parameters

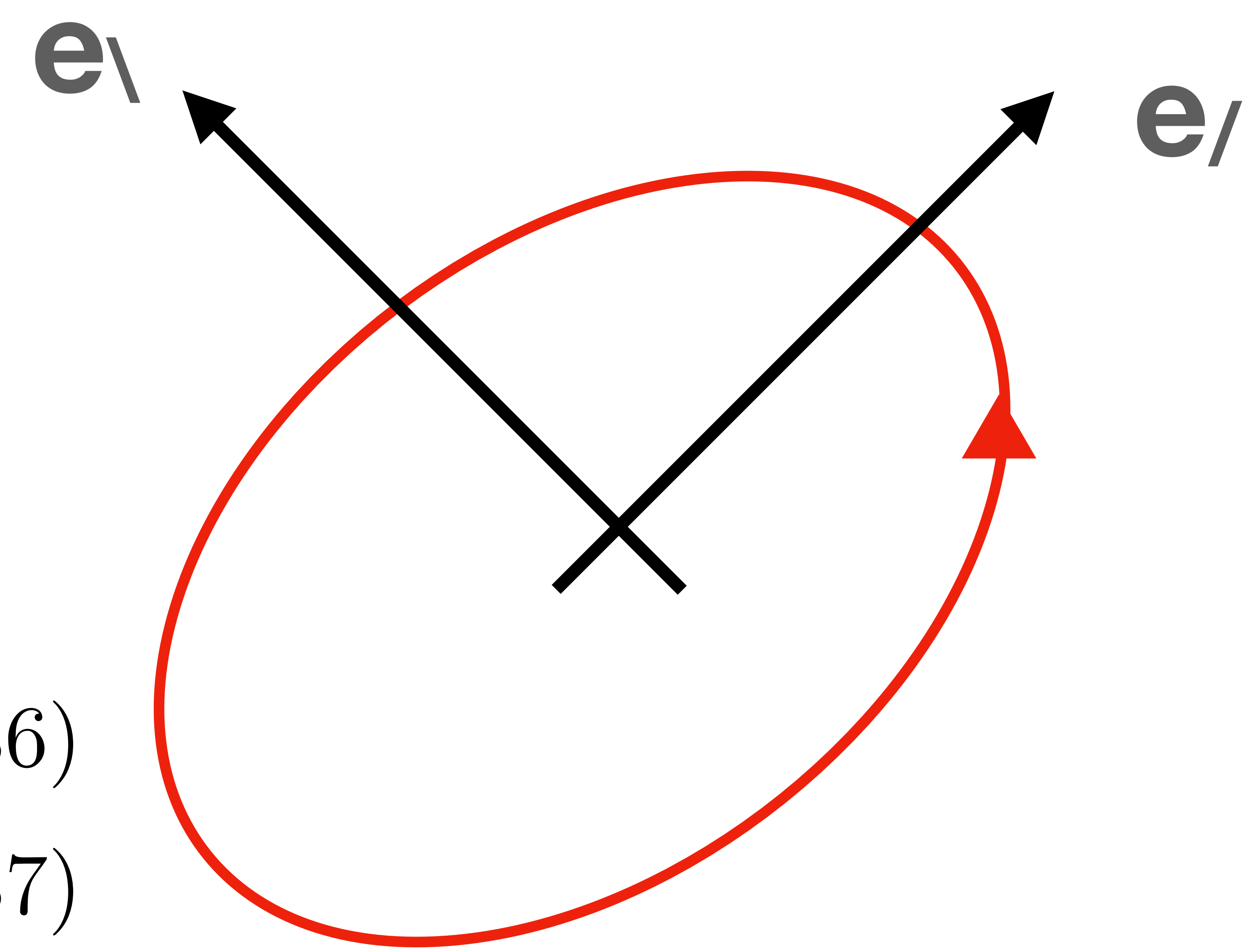

$$
\begin{aligned}
I &= \left|\mathbf{e}_{1,+,/} \cdot \mathbf{E}\right|^2 + \left|\mathbf{e}_{2,-,\backslash} \cdot \mathbf{E}\right|^2 && (1.36)\\
Q &= \left|\mathbf{e}_1 \cdot \mathbf{E}\right|^2 - \left|\mathbf{e}_2 \cdot \mathbf{E}\right|^2 && (1.37)\\
U &= \left|\mathbf{e}_/ \cdot \mathbf{E}\right|^2 - \left|\mathbf{e}_\backslash \cdot \mathbf{E}\right|^2 && (1.38)\\
V &= \left|\mathbf{e}_+^* \cdot \mathbf{E}\right|^2 - \left|\mathbf{e}_-^* \cdot \mathbf{E}\right|^2, && (1.39)
\end{aligned}
$$

$$
\begin{aligned}
\mathbf{e}_/ &= \frac{1}{\sqrt{2}}(\mathbf{e}_1 + \mathbf{e}_2)\\
\mathbf{e}_\backslash &= \frac{1}{\sqrt{2}}(\mathbf{e}_1 - \mathbf{e}_2)
\end{aligned}
$$

Stokes parameters - linear polarization

$$\mathbf{E}_p\left(\mathbf{x},t\right) = E_p\left(\mathbf{e}_1\cos\theta + \mathbf{e}_2\sin\theta\right)e^{i(\mathbf{k}\cdot\mathbf{x}-\omega t)}$$

$$Q = I_p\cos\left(2\theta\right) \tag{1.41}$$

$$U = I_p\sin\left(2\theta\right) \tag{1.42}$$

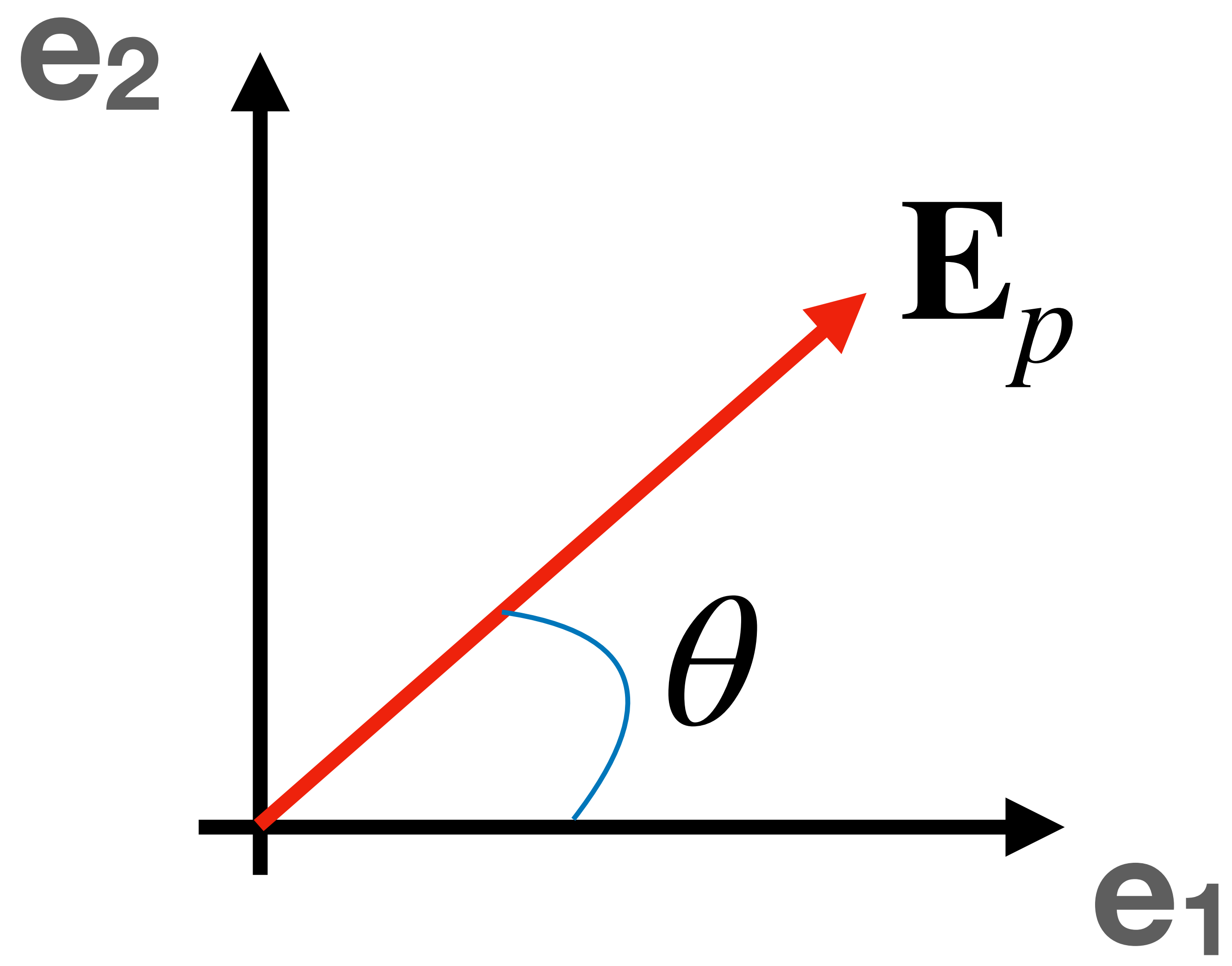

polarization fraction and angle

$$p = \frac{\sqrt{Q^2+U^2}}{I} \tag{1.43}$$

$$\theta = \frac{1}{2}\arctan\left(\frac{U}{Q}\right). \tag{1.44}$$

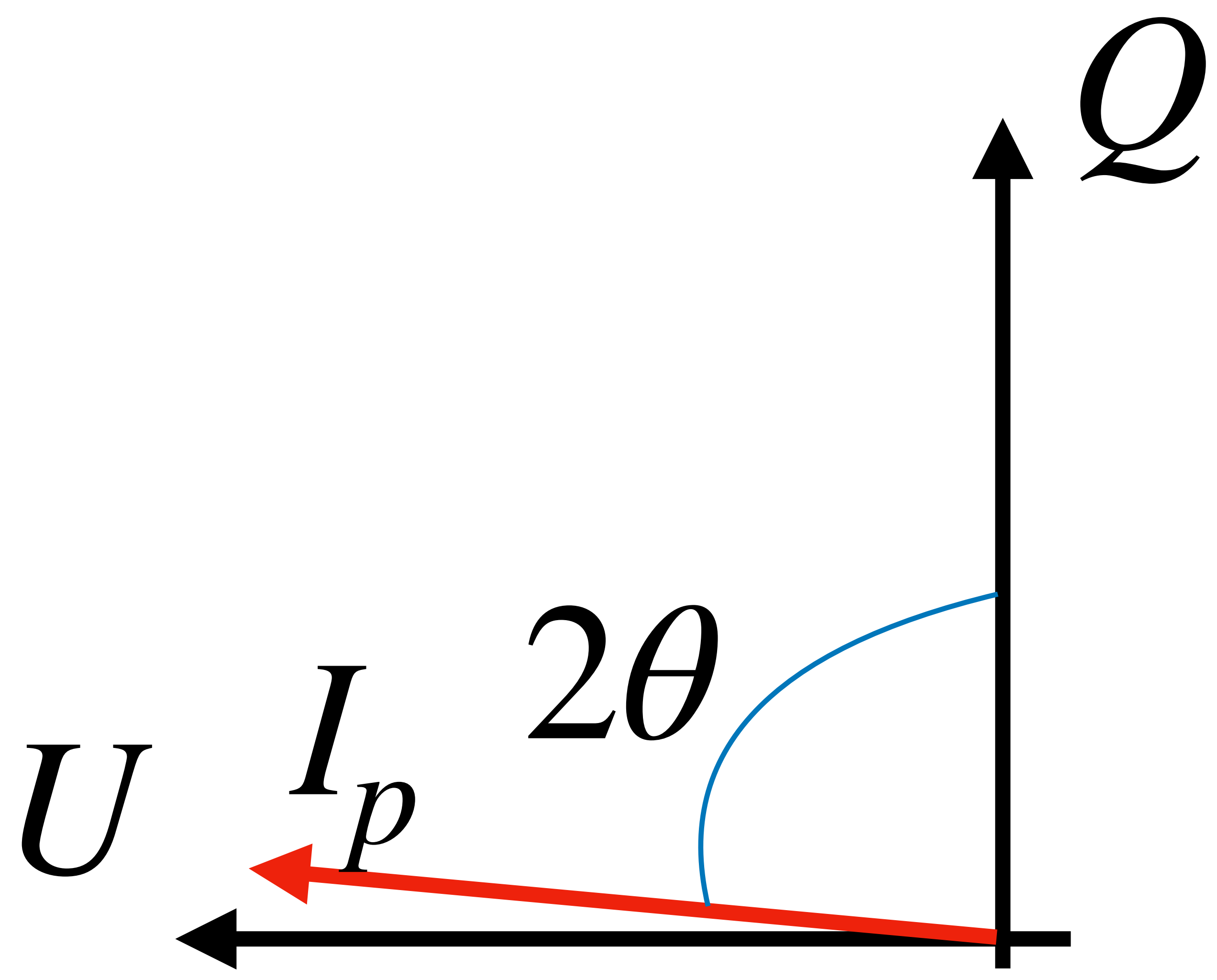

Stokes parameters - linear polarization

The combination of these two parameters lend themselves well to the notion of a **polarization (pseudo-)vector**, where the length of the vector is set by p and its orientation (which is not a direction) by θ. One must, however, by careful with this analogy because these pseudo-vectors do not behave like normal vectors. For example,

- two polarization measurements yielding the same level p and orientations differing by $\pi/2$ do not add up to give a total vector of length $\sqrt{2}p$ and of intermediate orientation. Instead equations (1.41)-(1.42) make it clear the resulting polarization pseudo-vector will be of length $p = 0$ since $\cos(2\theta) + \cos(2\theta + \pi) = \sin(2\theta) + \sin(2\theta + \pi) = 0$. In other words, polarization pseudo-vectors exhibiting the same level p and orientated perpendicular to one another cancel out.
- Although p and θ lend themselves well for certain types of analysis, it is important to remember that Q and U are the fundamental quantities that should be manipulated for calculations performed at the fundamental level. For example, if two sets of polarization measurements made on the same source are to be combined to, say, improve the signal-to-noise ratio, then it is the Q and U parameters that must be averaged, not p and θ.

Polarization from spectral lines

$\Rightarrow$ *Individual spectral lines from atoms or molecules are intrinsically polarized, but...* $\Leftarrow$

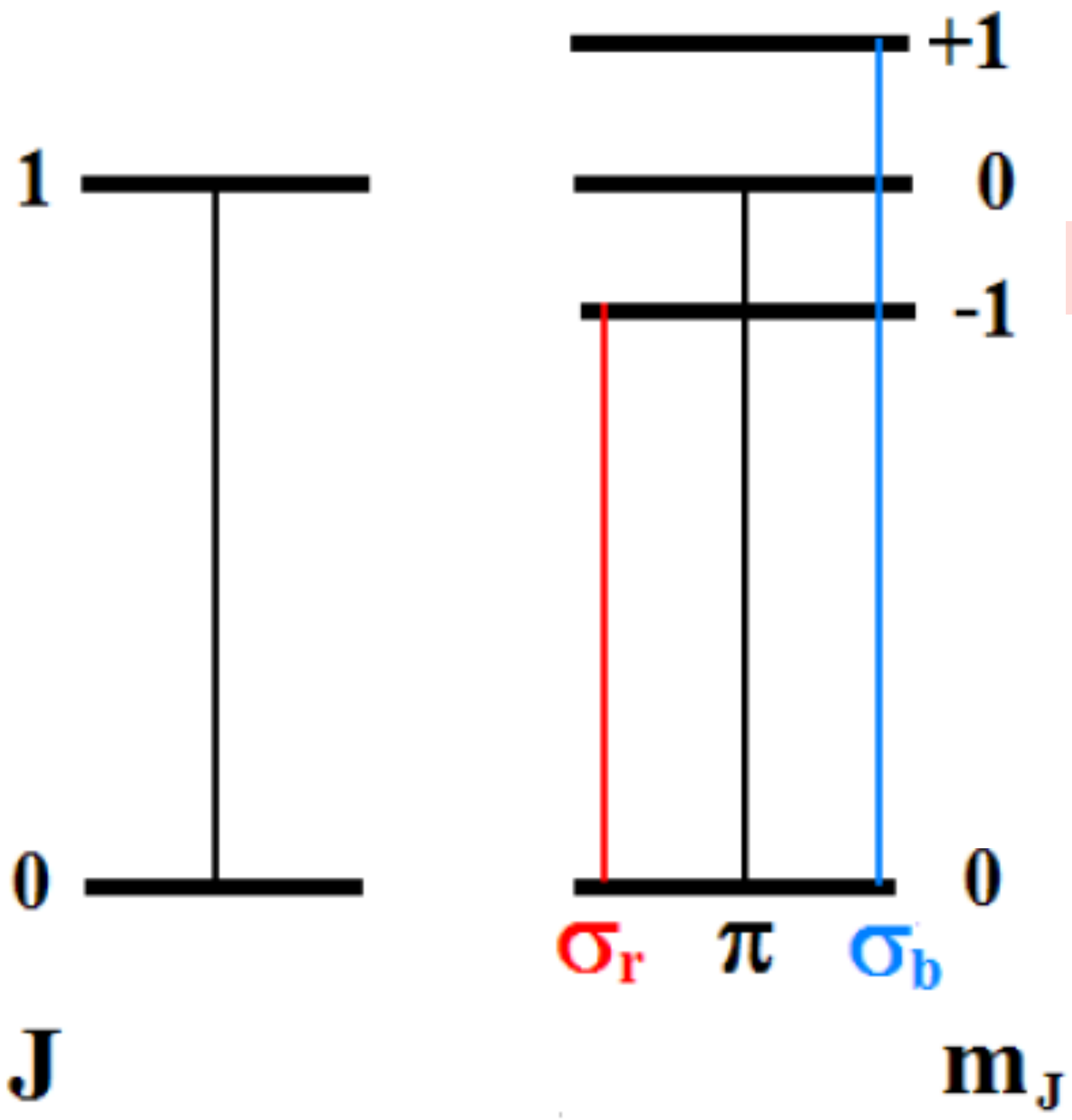

Let us consider the case, for example, of a simple molecule (e.g., as carbon monoxide (CO)) with rotational states $|J, m\rangle$ defined by the quantum numbers J and m, with $-J \leq m \leq J$ in steps of 1. We will assume, for simplicity, that the molecule is in the electronic and vibrational ground states such that we are only dealing with pure rotational transitions. A transition $|J, m\rangle \rightarrow |J + \Delta J, m + \Delta m\rangle$ will be allowed for cases where $\Delta J = \pm 1$ and $\Delta m = 0, \pm 1$; an example is provided in Figure 1.1. The nature of

Polarization from spectral lines - alignment

A group of atoms or molecules must somehow be aligned in order to exhibit detectable polarized emission (or absorption) from a given spectral line, i.e., their symmetry axis must have a preferential orientation in relation to some external agent. An ambient magnetic field pervading the region within which the atoms/molecules are located will serve such a purpose, as long as a few conditions are met:

- The atoms/molecules under question are endowed with a magnetic moment. Certainly, this will be the case for molecules to soon be discussed within the context of the Zeeman effect (e.g., HI, OH and CN) since, as we will see, the frequency splitting at the heart of this effect comes from a magnetic dipolar interaction. However, even other molecules weakly sensitive to the Zeeman effect (e.g., CO, CS, H_2O, ...) will also have a small magnetic moment due to the rotation of their nuclei (and their "slipping" from the electrons).

- If the magnetic moment μ and the ambient magnetic field strength B are such that $\mu B/\hbar > \nu_{\text{coll}}, A_{ul}, B_{ul}I$, with ν_{coll} the collisional rate and A_{ul} and $B_{ul}I$ the spontaneous and stimulated emission rates, then the molecules will be effectively aligned by the magnetic field. This condition usually easily met in a wide range of environments. For example, for molecules like CO we $\mu/\hbar \sim 1$ mH/μG while at a density of, say, $n \sim 10^4$ cm^{-3} and a relative collision velocity of $\Delta v \sim 1$ km/sec $\nu_{\text{coll}} \approx n\sigma\Delta v \approx 10^{-6}$ s^{-1} (i.e., $\sigma \sim 10^{-15}$ cm^2), as well $A_{ul} \sim 10^{-6}$ s^{-1} for CO $(J = 2 \to 1)$. That is, even a weak magnetic field of $B \sim 10$ μG will easily meet this condition.

Polarization from spectral lines - alignment

- The π-line (when $\Delta m = 0$) only emits linearly polarized radiation aligned with the external magnetic field and a radiation pattern perpendicular to it. For example, an observer detecting emission from a π-line when the external magnetic field is confined to the plane of the sky would see the corresponding spectral line as being linearly polarized in the same direction as the field. On the other hand, the π-line would not be detected if the magnetic field was (anti-)parallel with the line of sight. At intermediate orientation for the magnetic field, the radiation from the π-line would be polarized along the orientation of the projected magnetic field on the plane of the sky.

- Radiation from the σ-lines (when $\Delta m = \pm 1$) is generally elliptically polarized, with their common linear polarization component perpendicular to that of the π-line (i.e., perpendicular to the orientation of the projected magnetic field on the plane of the sky). The two σ-lines have, however, opposite circular polarization states (i.e., right for $\Delta m = +1$ and left for $\Delta m = -1$ when the field is pointing at the observer, and vice-versa). The detected polarization for a given σ-line is purely linear when the magnetic field is confined to the plane of the sky and purely circular (anti-)parallel with the line of sight.

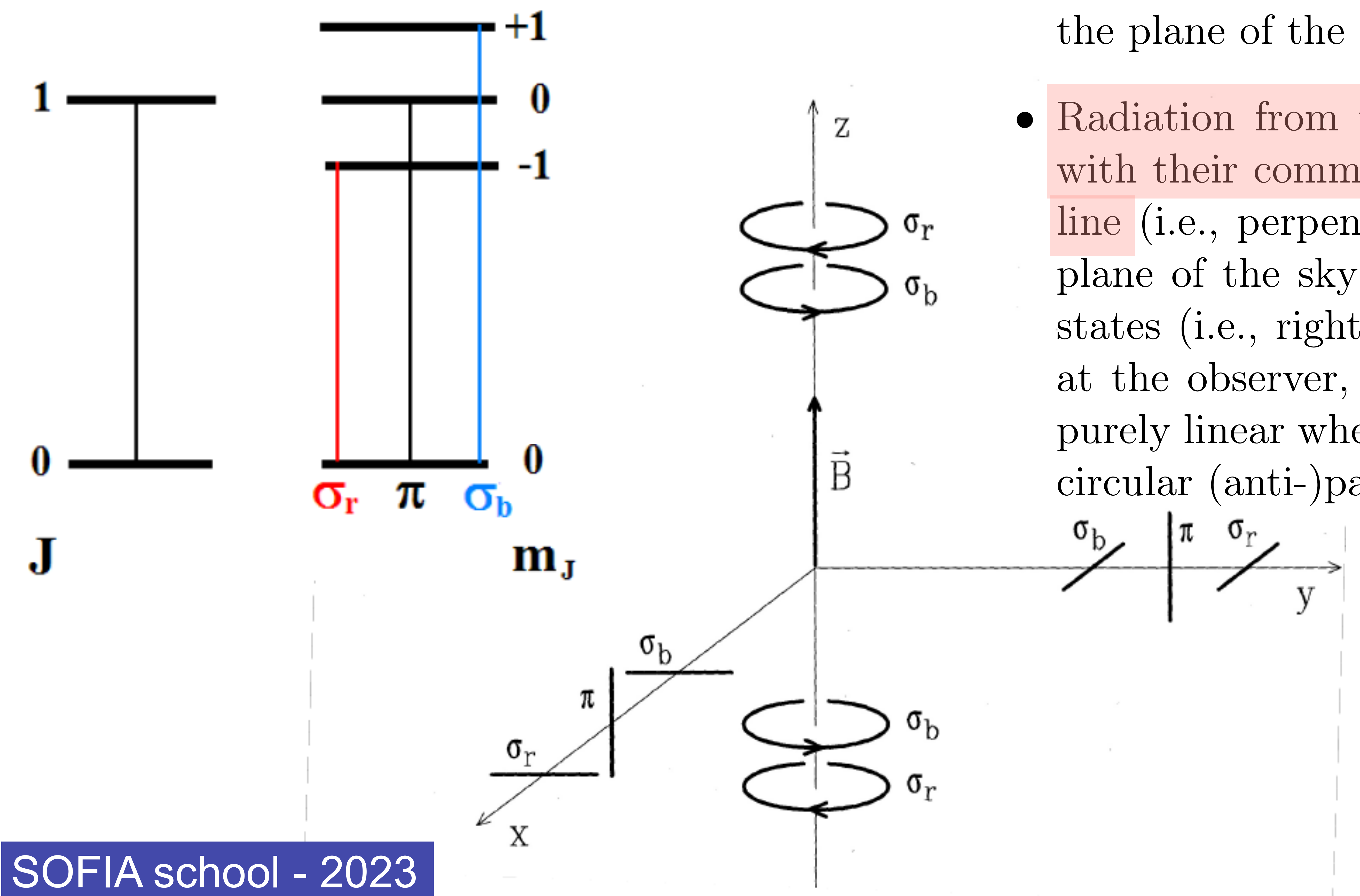

Polarization from spectral lines - alignment

$\Rightarrow$ *Individual spectral lines from atoms or molecules are intrinsically polarized, but...* $\Leftarrow$

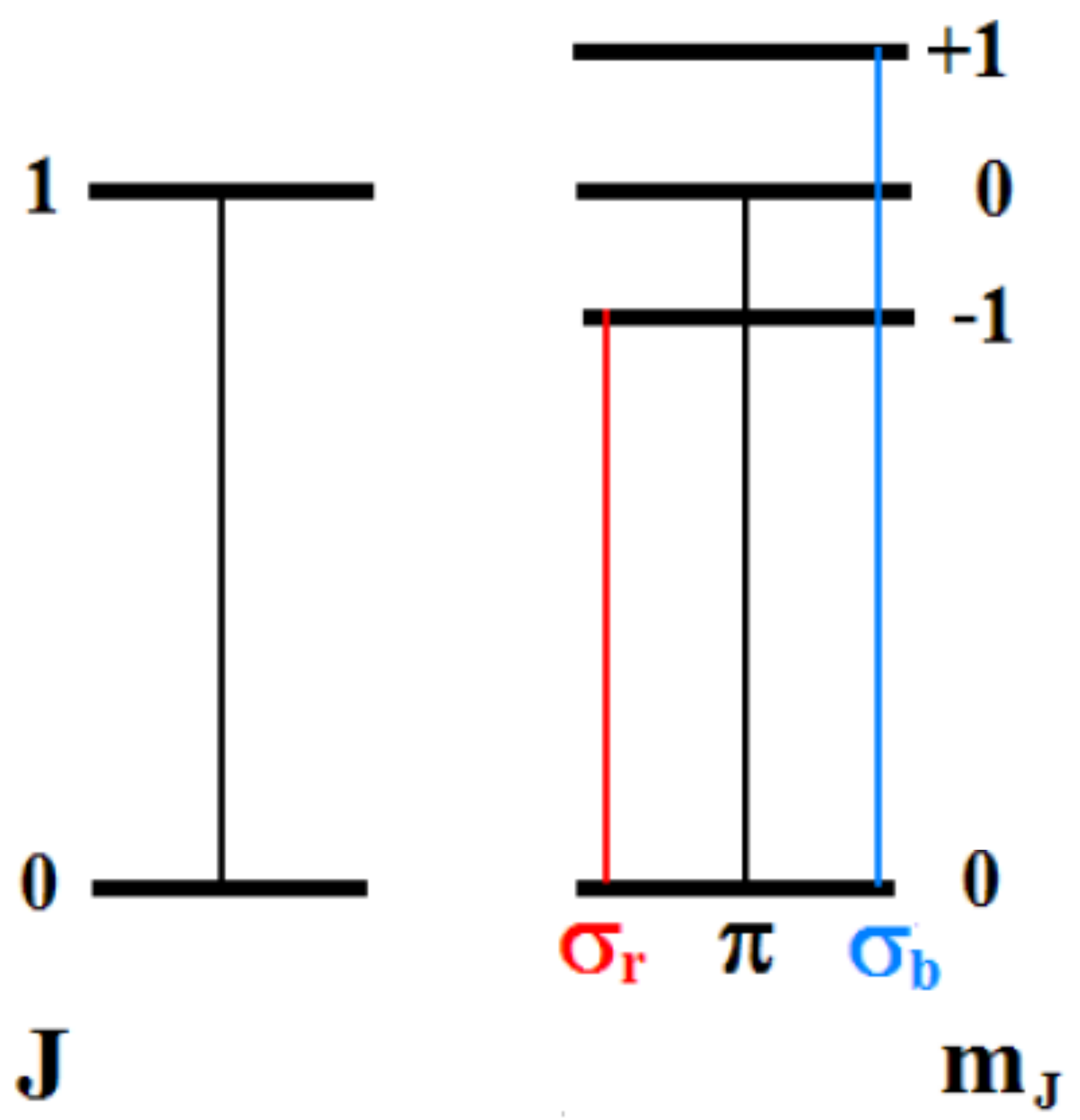

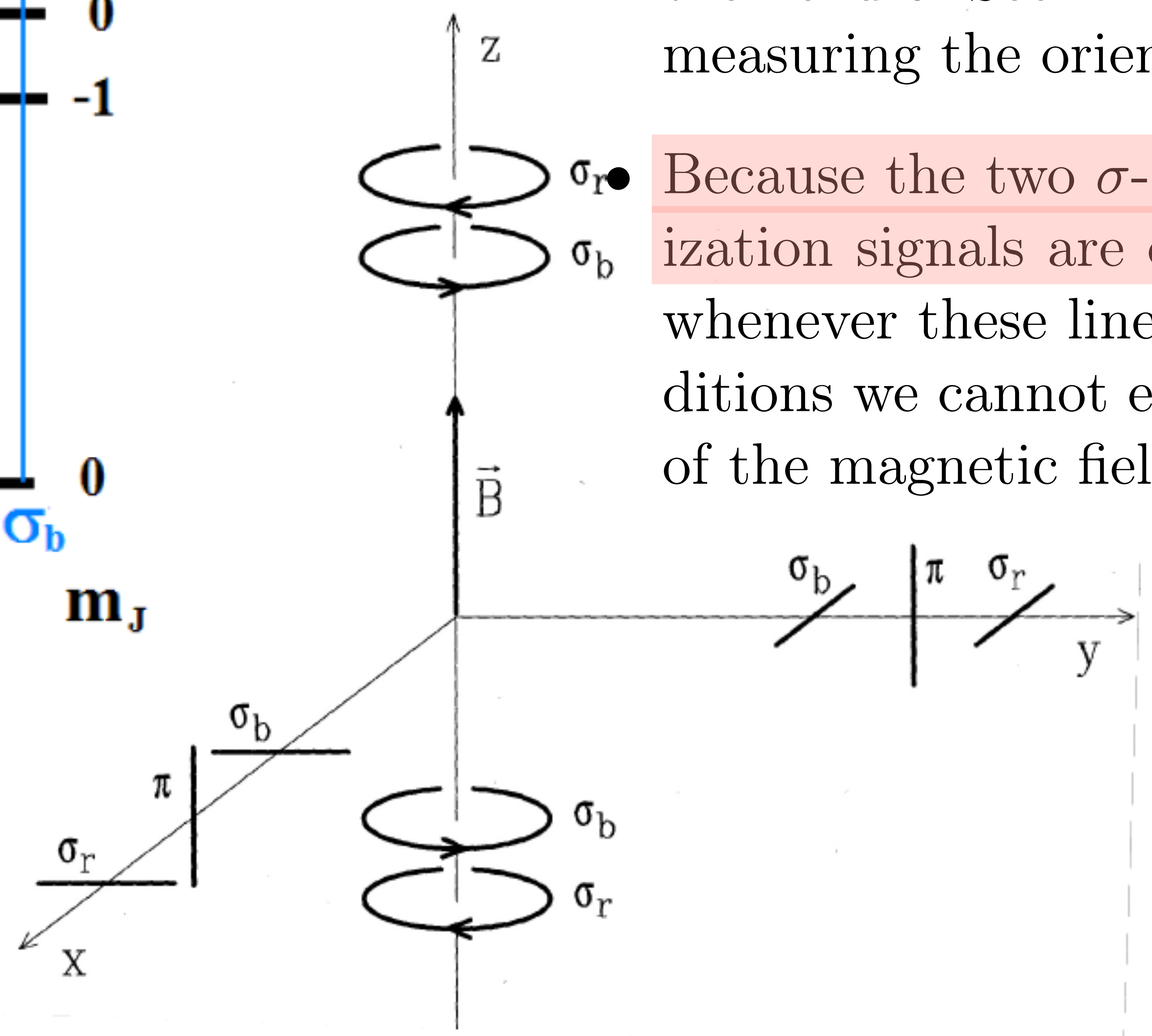

- At thermodynamic equilibrium both σ-lines have the same intensity and their total intensity equals that of the π-line. If all these lines happen at the same (or are close in) frequency, then their polarization pseudo-vectors will cancel out because there would then be an equal intensity or radiation in perpendicular radiation states (see then end of Sec. 1.1). The lack of a polarization signal implies the impossibility of measuring the orientation of the projected magnetic field on the plane of the sky.
- Because the two σ-lines share the same radiation pattern and their circular polarization signals are opposite (i.e., orthogonal) no net polarization can be detected whenever these lines fall at the same (or are close in) frequency. Under these conditions we cannot expect to learn anything concerning the line of sight component of the magnetic field.

Spectral lines - external magnetic field

$$\begin{aligned}\hat{H} &= \hat{H}_0 - \hat{\boldsymbol{\mu}} \cdot \mathbf{B} \\ &= \hat{H}_0 - \frac{\mu_\mathrm{B}}{\hbar} \hat{L}_z B, \end{aligned} \tag{1.49}$$

$$\Delta E_{\ell,m} = -\mu_\mathrm{B} m B. \tag{1.50}$$

We therefore find that the energy of the system is altered by a quantity that is proportional to the **magnetic quantum number** m and the external magnetic field. This

Spectral lines - external magnetic field

$$\hat{H} = \hat{H}_0 - \hat{\boldsymbol{\mu}} \cdot \mathbf{B}$$
$$= \hat{H}_0 - \frac{\mu_\mathrm{B}}{\hbar} \hat{L}_z B, \qquad (1.49)$$

$$\Delta E_{\ell,m} = -\mu_\mathrm{B} m B. \qquad (1.50)$$

We therefore find that the energy of the system is altered by a quantity that is proportional to the **magnetic quantum number** m and the external magnetic field. This

Degeneracy is lifted!

Spectral lines - Zeeman effect

Before we look more closely at some candidate spectral lines, let us look at what can be expected as far as solving our frequency degeneracy problem. The Zeeman sensitivity associated with these spectral transitions is on the order of 1 Hz/μG. Looking on the high-side of magnetic field strengths we can expect $B \sim 1$ mG in the denser parts of giant molecular clouds. That is, the **Zeeman splitting** between the π- and σ-lines will be $\Delta\nu_z \sim 1$ kHz. On the other hand, line of sight velocities measured for these spectral lines can often reach as high as tens of km/s. Using the Doppler shift formula we find that

$$\Delta\nu \approx 3.3 \left(\frac{\nu_0}{1\ \mathrm{GHz}}\right)\left(\frac{\Delta v}{1\ \mathrm{km\,s^{-1}}}\right)\ \mathrm{kHz}, \tag{1.52}$$

where ν_0 and Δv are the frequency of the spectral transition and its line width, respectively.

We can therefore already see that, although π- and σ-lines will not fall on the same frequency for a given line of sight velocity, there will be significant spectral overlap between them. This effect, which gets worse with increasing frequency, will strongly limit the applicability of the Zeeman effect for measuring the magnetic field strength. For example, while the Doppler broadening would be on the order ~ 5 kHz with $\Delta v = 1$ km/s for the commonly used OH lines at 18 cm, it would become ~ 376 kHz for the CN $(N = 1 \rightarrow 0)$ transition at 113 GHz.

Spectral lines - Zeeman effect

$$Q \simeq -\frac{1}{4}\frac{d^2 I}{d\nu^2}\left(\cos\theta - \sin\theta\right)\left(\Delta\nu_z \sin\iota\right)^2 \quad (1.53)$$

$$U \simeq -\frac{1}{4}\frac{d^2 I}{d\nu^2}\left(\sqrt{2}\sin\theta\right)\left(\Delta\nu_z \sin\iota\right)^2 \quad (1.54)$$

$$V \simeq \frac{dI}{d\nu}\Delta\nu_z \cos\iota, \quad (1.55)$$

with θ, as before, the polarization angle on the plane of the sky (relative to $\mathbf{e}_1$) and ι the inclination angle of the magnetic field relative to the line of sight (Crutcher et al. 1993, ApJ, 407, 175). It follows that

Spectral lines - Zeeman effect

$$Q \simeq -\frac{1}{4}\frac{d^2I}{d\nu^2}\left(\cos\theta - \sin\theta\right)\left(\Delta\nu_z \sin\iota\right)^2 \tag{1.53}$$

$$U \simeq -\frac{1}{4}\frac{d^2I}{d\nu^2}\left(\sqrt{2}\sin\theta\right)\left(\Delta\nu_z \sin\iota\right)^2 \tag{1.54}$$

$$V \simeq \frac{dI}{d\nu}\Delta\nu_z \cos\iota, \tag{1.55}$$

with θ, as before, the polarization angle on the plane of the sky (relative to $\mathbf{e}_1$) and ι the inclination angle of the magnetic field relative to the line of sight (Crutcher et al. 1993, ApJ, 407, 175). It follows that

HI 21 cm - Zeeman effect

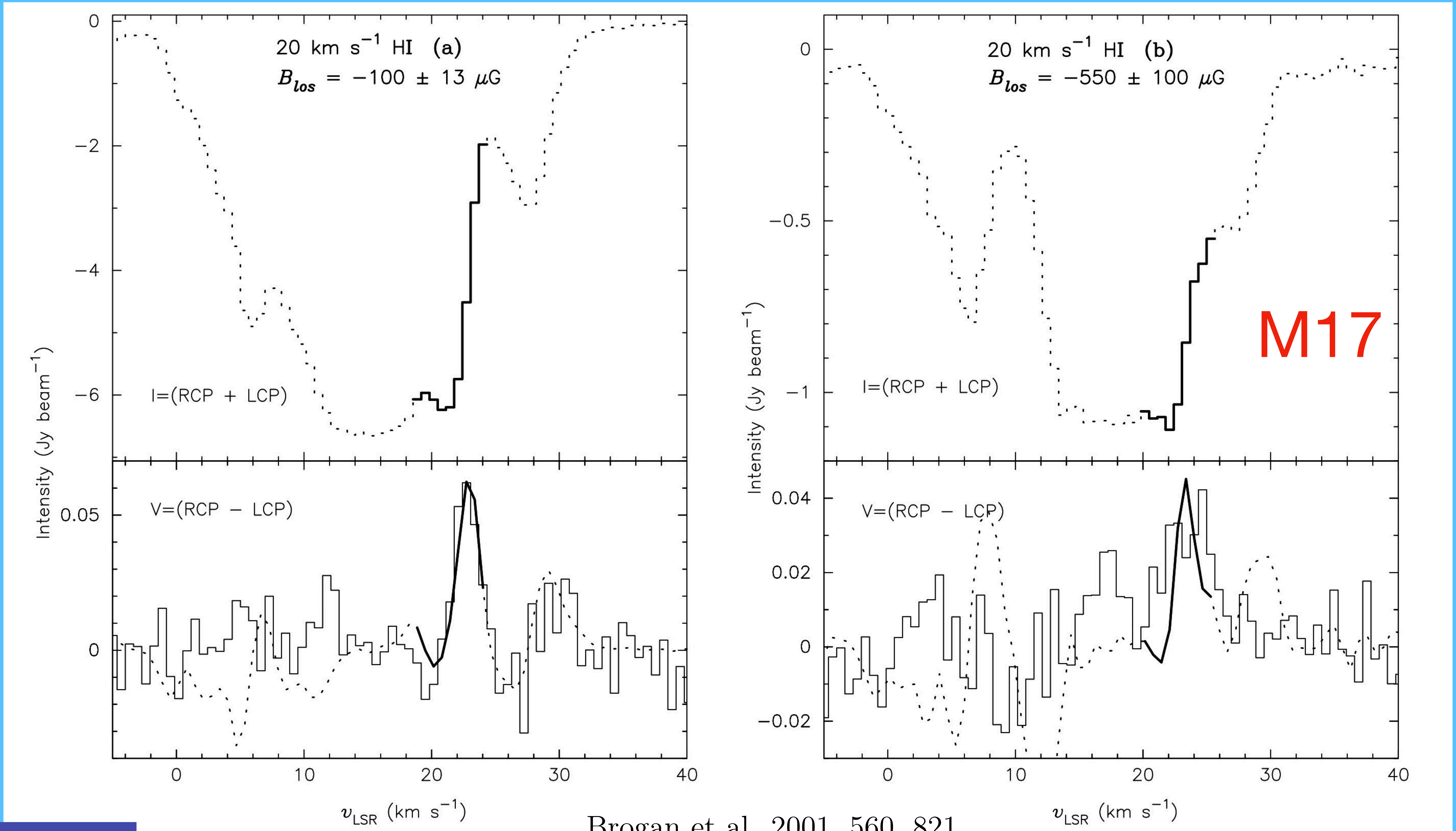

Brogan et al. 2001, 560, 821

OH 18 cm & CN (J=5-4)- Zeeman effect

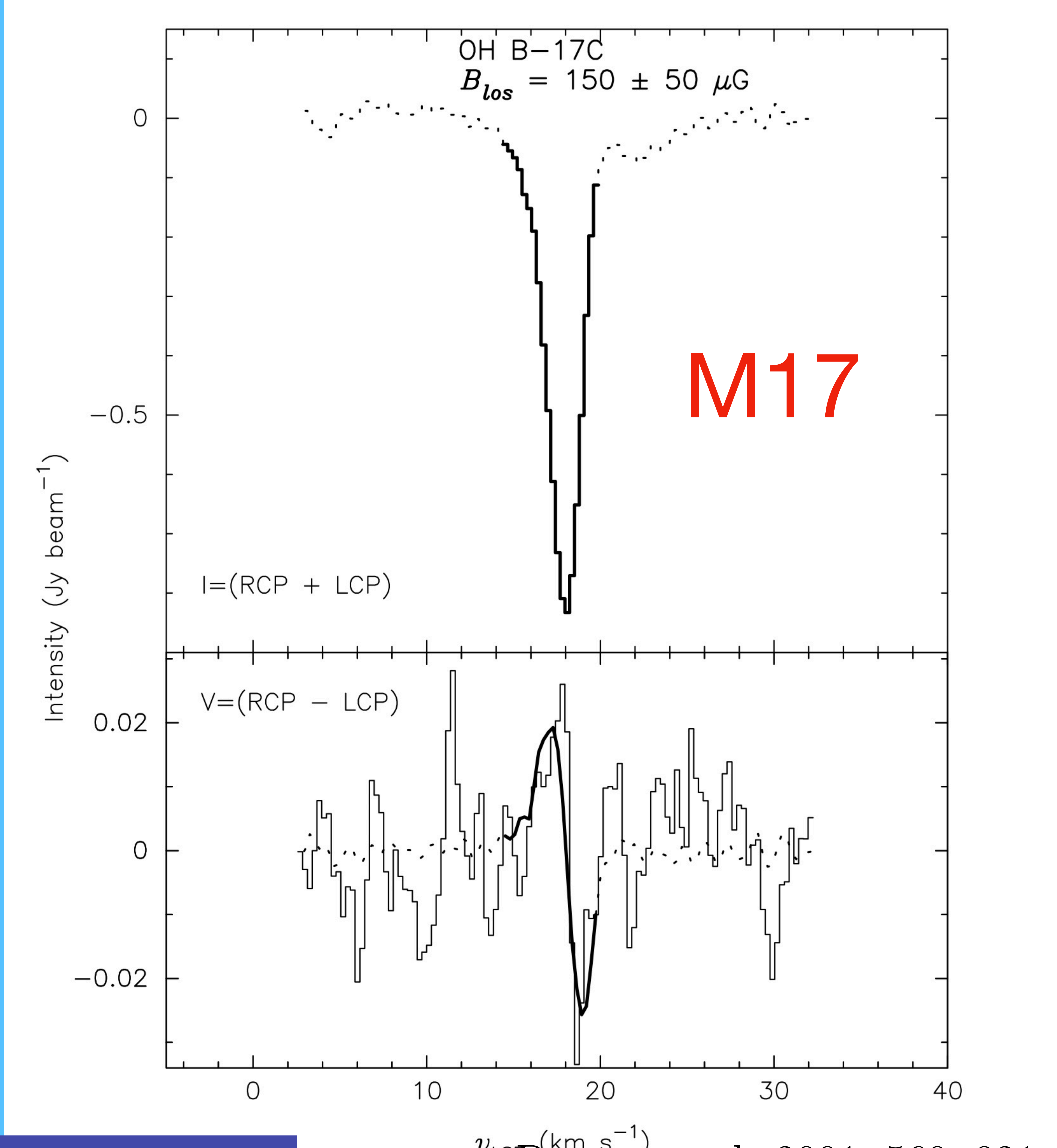

Brogan et al. 2001, 560, 821

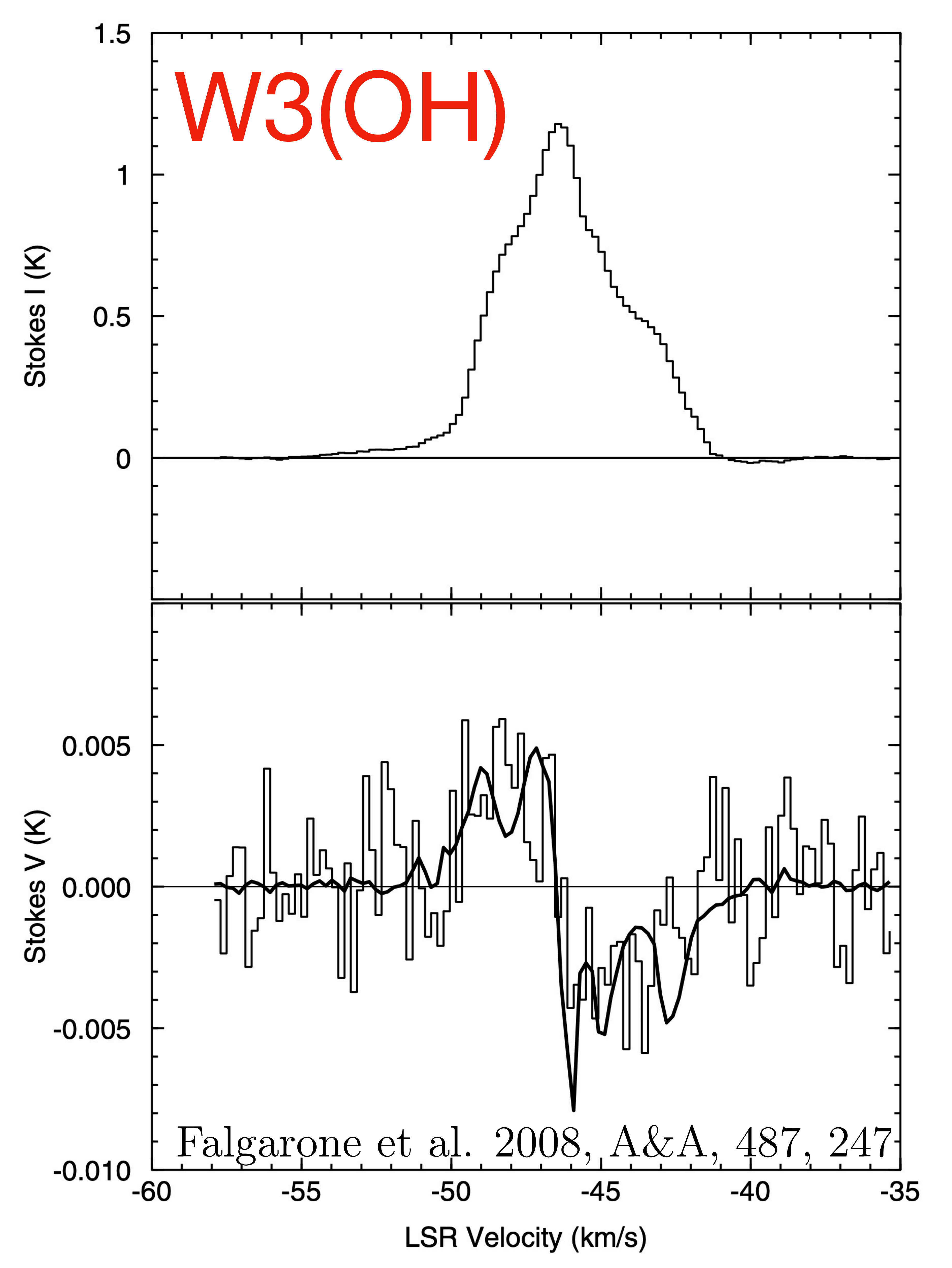

Falgarone et al. 2008, A&A, 487, 247

Spectral lines - Zeeman effect

Zeeman Results - log B_{los} *vs.* log N(H)

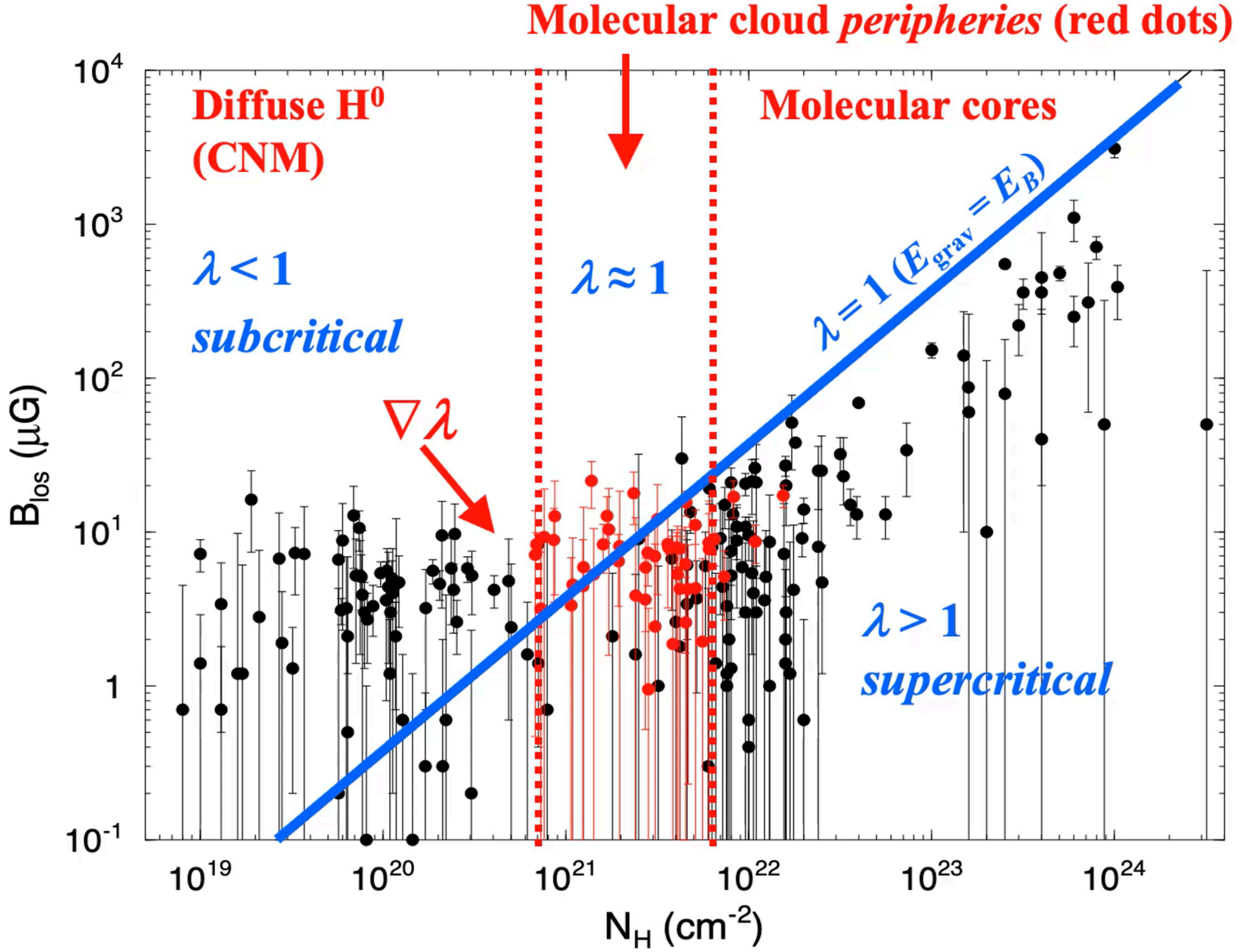

5. Summary

- **Existing Zeeman effect data on B_{los} cover wide ranges:**
  - N(H) = 10^{19} - 10^{24} cm^{-2} ($A_v \approx$ 0.005 - 500)
  - n(H) = 10 - 10^6 cm^{-3}
- **Data suggest transformation from diffuse, *magnetically dominated* ISM into *gravitationally dominated* ISM at these critical values**
  - N_0(H) ≈ 10^{22} cm^{-2}
  - n_0(H) ≈ 300 cm^{-3}
  - L_0 = N_0(H) / n_0(H) ≈ 10 pc (approximate Jeans length for the CNM)
- **Data suggest ISM is in near equipartition between magnetic and turbulent energies, with turbulence slightly sub-Alfvenic.**

Courtesy T. Troland, adapted from Crutcher et al. 2010, ApJ, 725, 466.

Spectral lines - Zeeman effect & masers

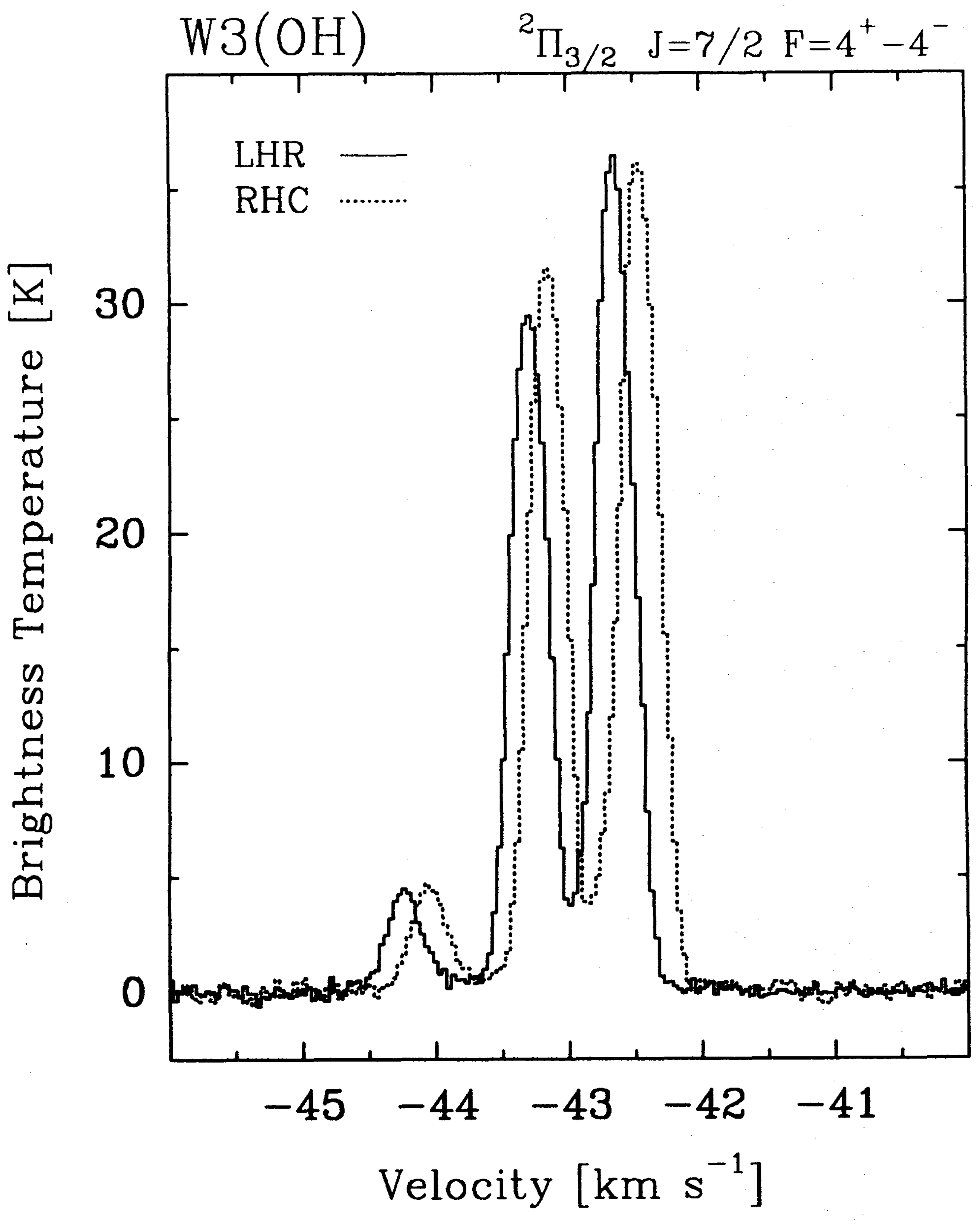

Figure 1.8: Detection of the Zeeman effect in OH $\left({}^2\Pi_{3/2}, J = 7/2, F = 4^+ \rightarrow 4^-\right)$ lines in the W3(OH) molecular cloud complex. The combination of narrow spectral lines ($\Delta v \approx 0.3\,\mathrm{km\,s^{-1}}$ or ≈ 13 kHz) and strong *total* magnetic fields ($B \simeq 7.6 - 10.6$ mG) resulted in a clear Zeeman splitting $\Delta\nu_z \simeq 6 - 8.4$ kHz. From Güsten, Fiebig and Uchida 1994, A&A, 26, L51.

Spectral lines - Zeeman effect & masers

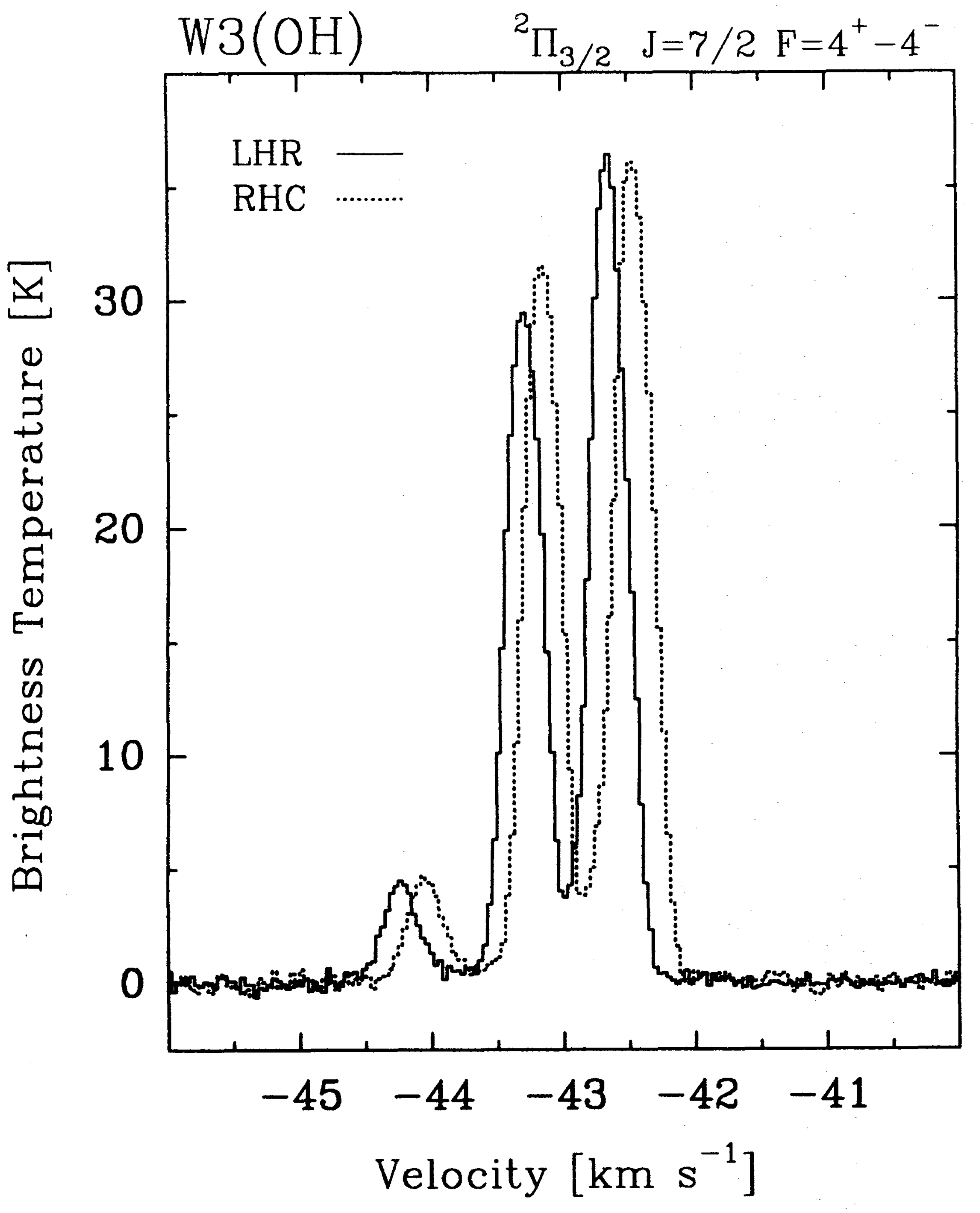

"... a bow-shock model in which the magnetic field is compressed in the cooled post-shock layer preceding the compact HII region. "

Figure 1.8: Detection of the Zeeman effect in OH $\left({}^2\Pi_{3/2}, J = 7/2, F = 4^+ \rightarrow 4^-\right)$ lines in the W3(OH) molecular cloud complex. The combination of narrow spectral lines ($\Delta v \approx 0.3\,\mathrm{km\,s^{-1}}$ or ≈ 13 kHz) and strong *total* magnetic fields ($B \simeq 7.6 - 10.6$ mG) resulted in a clear Zeeman splitting $\Delta\nu_z \simeq 6 - 8.4$ kHz. From Güsten, Fiebig and Uchida 1994, A&A, 26, L51.

Polarization from spectral lines - Goldreich-Kylafis

- Most molecules/transition —> no Zeeman effect
  - E.g., CO is more than 1000 times less sensitive to Zeeman than CN
- π- and σ-lines will fall at the same frequency
- How to get linear polarization?
  - Move away from thermodynamics equilibrium because the π- and σ-lines will cancel each other
  - Anisotropy will bring linear polarization (no circular polarization)
    - E.g., velocity gradient or increased optical depth along magnetic field, anisotropic external radiation field, …
  - No information on magnetic field strength
  - 90 deg ambiguity

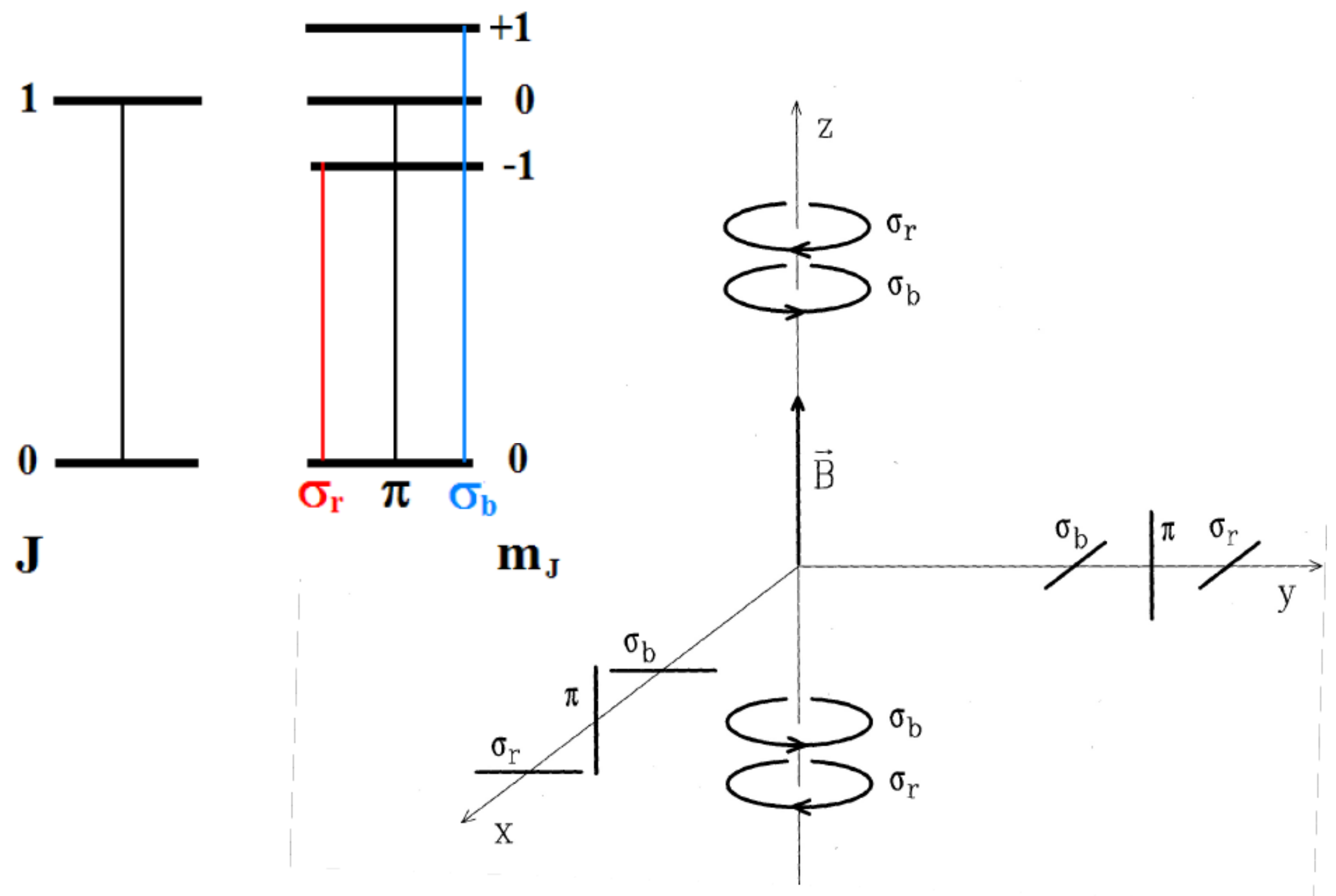

Polarization from spectral lines - Goldreich-Kylafis

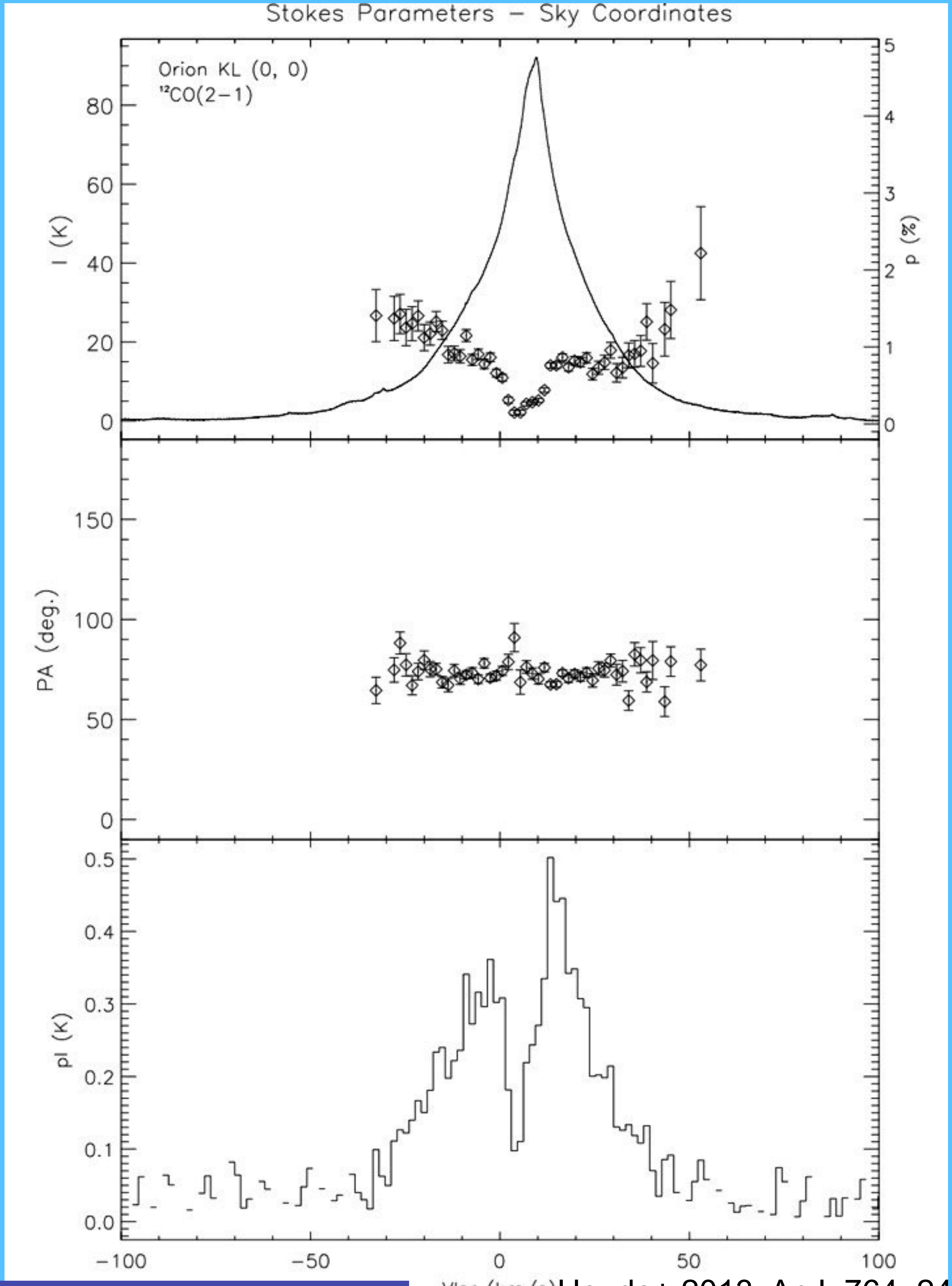

Houde+ 2013, ApJ, 764, 24

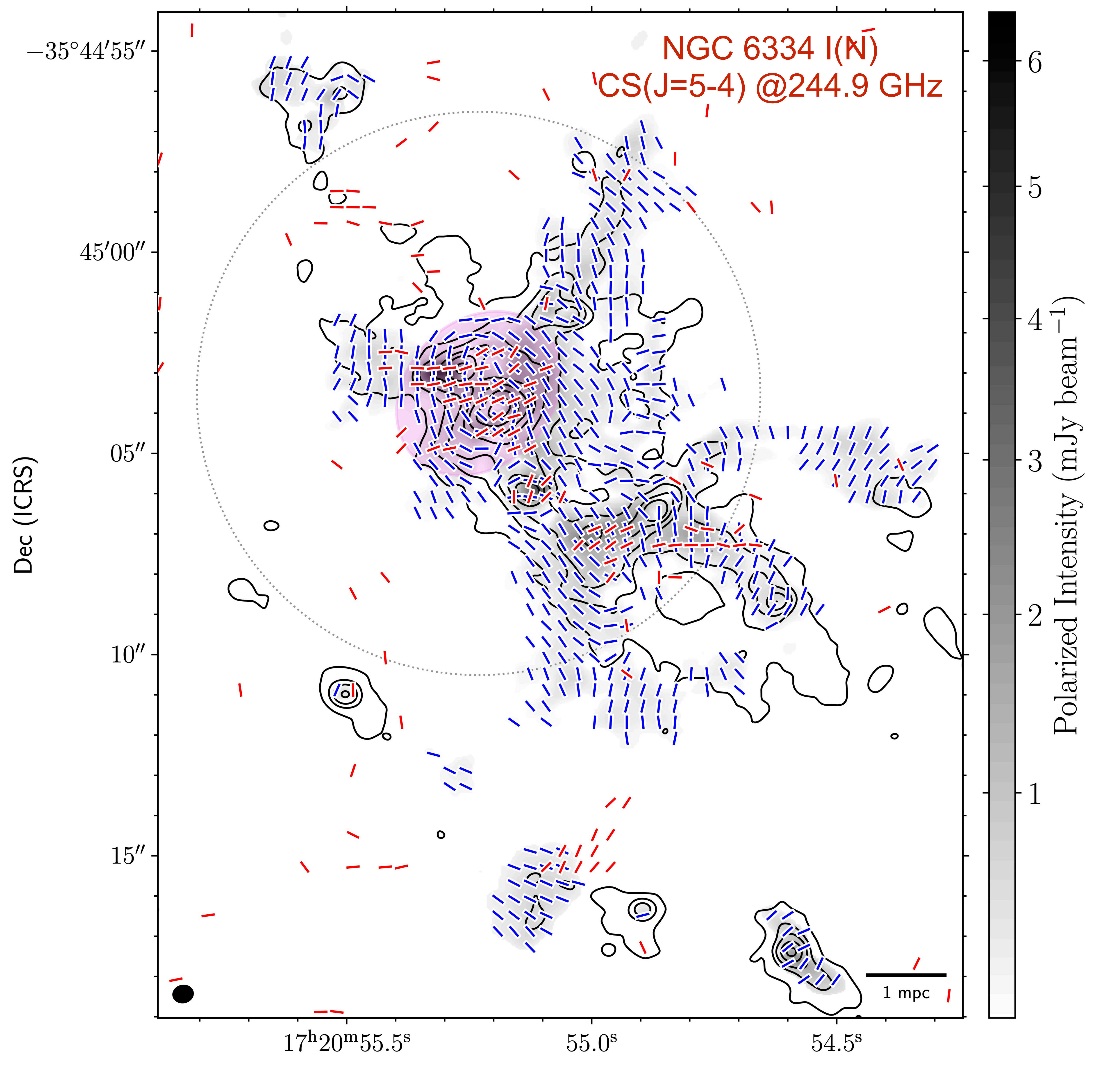

Cortés+ 2021, ApJ, 923, 204

Spectral lines - Goldreich-Kylafis + masers

Measuring magnetic fields from water masers in the synchrotron protostellar jet in W3(H_2O)

C. Goddi[1,2], G. Surcis[3,4], L. Moscadelli[5], H. Imai[6], W. H. T. Vlemmings[7], H. J. van Langevelde[3,8], and A. Sanna[9]

Goddi et al. 2017, A&A, 597, A43

Spectral lines - Goldreich-Kylafis + masers

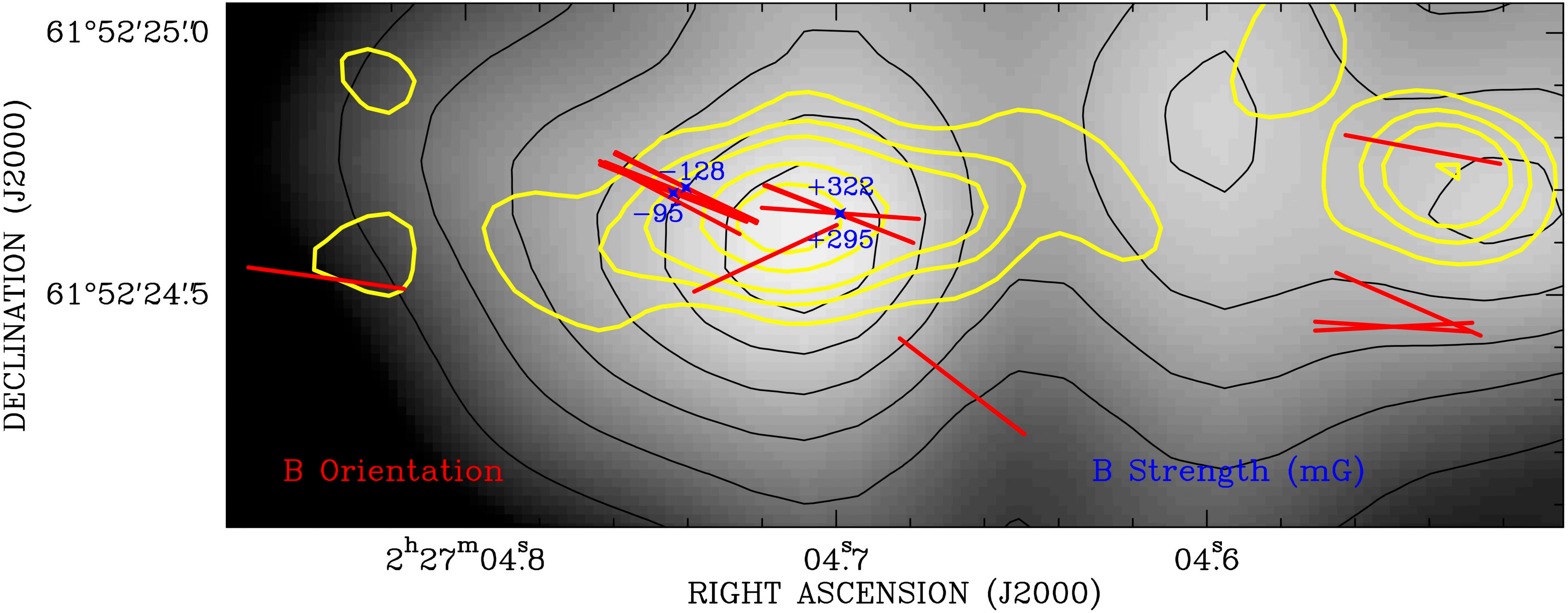

Fig. 2. Magnetic field orientation (in the plane of the sky) for 17 individual masers with $P_l < 5\%$ (red segment) and strength for four (non-saturated) masers for which the Zeeman splitting was measured. The 8.4 GHz emission imaged with the VLA (beamsize ~ 0.″2) by Wilner et al. (1999) (yellow contours: corresponding to 0.02, 0.06, 0.1, 0.2, 0.3 mJy beam^{-1}) is overplotted onto the 1.4 mm continuum emission mapped with the PdBI (beamsize ~ 0.″5) by Wyrowski et al. (1999) (gray scale and black contours: same as in Fig. 1). The radio continuum shows a main central component, the synchrotron jet, and two (western and eastern) secondary components (see Sect. 4.1 for an interpretation).

Goddi et al. 2017, A&A, 597, A43

Spectral lines - Goldreich-Kylafis + masers

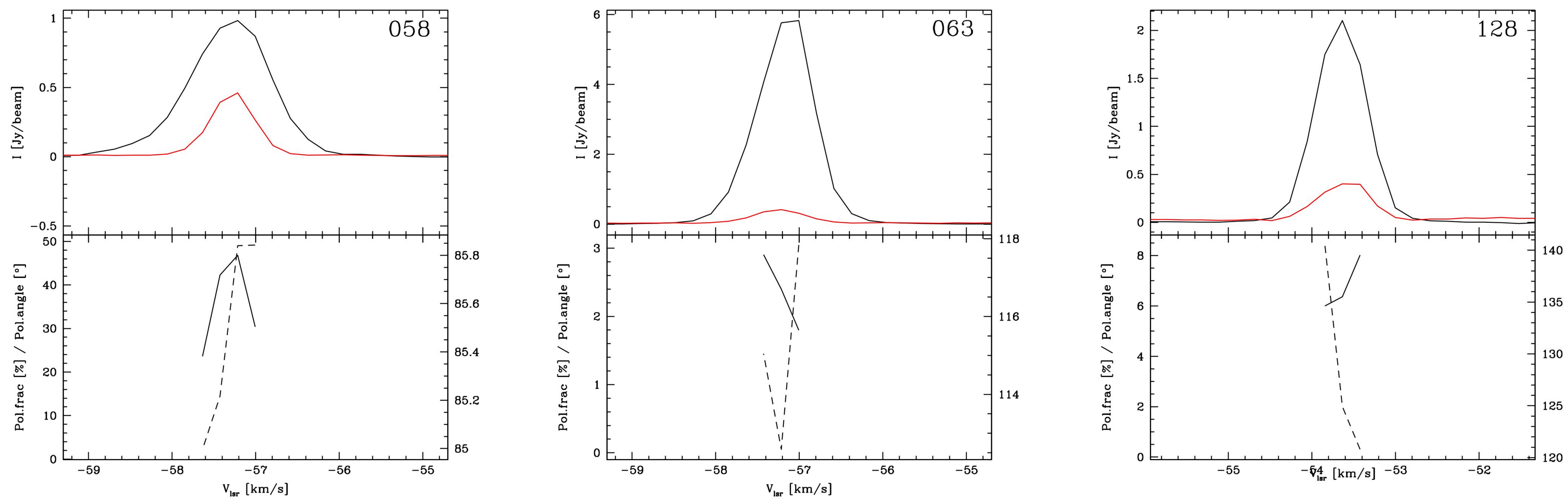

Fig. A.1. Total intensity (*I*, black solid line) and linear polarization intensity (red solid line) spectra of the H_2O maser features 012, 016, 036, 058, 063, and 128 (*upper panel*). The linear polarization intensity spectra have been multiplied by a factor of three for 036, 063, and 128. The linear polarization fraction (black solid line, left scale) and the linear polarization angle (dashed black line, right scale) are also shown (*lower panel*).

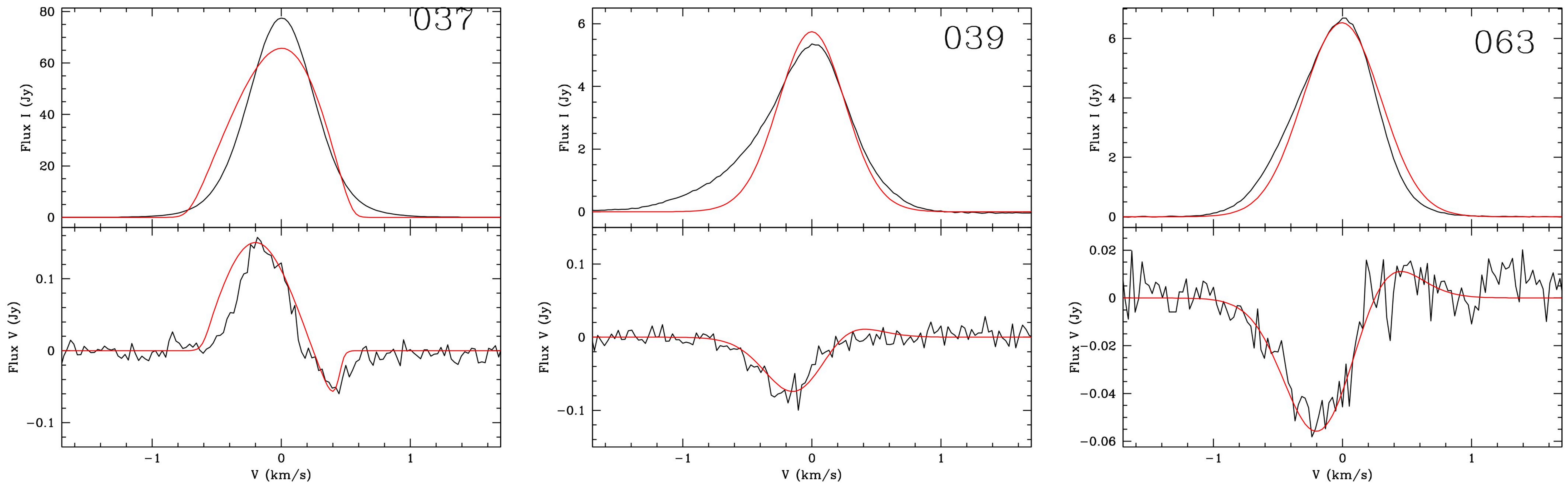

Fig. A.2. Total intensity (*I*, *upper panel*) and circular polarization intensity (*V*, *lower panel*) spectra for the H_2O maser features 037, 039, 063. The thick red line shows the best-fit models of *I* and *V* emission obtained using the FRTM code (see Appendix A). The maser features are centered on zero velocity.

Goddi et al. 2017, A&A, 597, A43

Polarization from dust - alignment

Just as was the case for molecules discussed earlier, a population of grains can only radiate globally with a net level of polarization if its constituents are somehow aligned with some external agent. Here again, the external magnetic field will fulfill this role. The leading theory for grain alignment is the so-called Radiative Alignment Torque (RAT) theory (Lazarian & Hoang 2007, MNRAS, 378, 910), and its main ingredients can be listed as follows:

- Within the framework of RAT irregularities in the shapes of dust grains lead to a finite helicity which will serve to spin them up when irradiated by an external radiation field (we saw from equations 1.6 and 1.8 that an electric field can be expressed with two orthogonal circularly polarized states, which will scatter differently off the grains because of their helicity).

- Once a grain is spinning it will tend do so by minimizing its total energy while conserving its angular momentum, resulting in a rotation about its symmetry axis (i.e., the "short" axis, which has the maximum moment of inertia). This is the so-called internal alignment process, which is rendered possible through the Barnett effect where quantum mechanical unpaired spins (we are dealing with paramagnetic grains) flip to make up for the change in rotational angular momentum in the alignment process.

- Since the flipping of spins also brings about a net magnetization (there are initially as many pointing up than down), the grain will interact with the external magnetic field, resulting in its symmetry axis precessing about it.

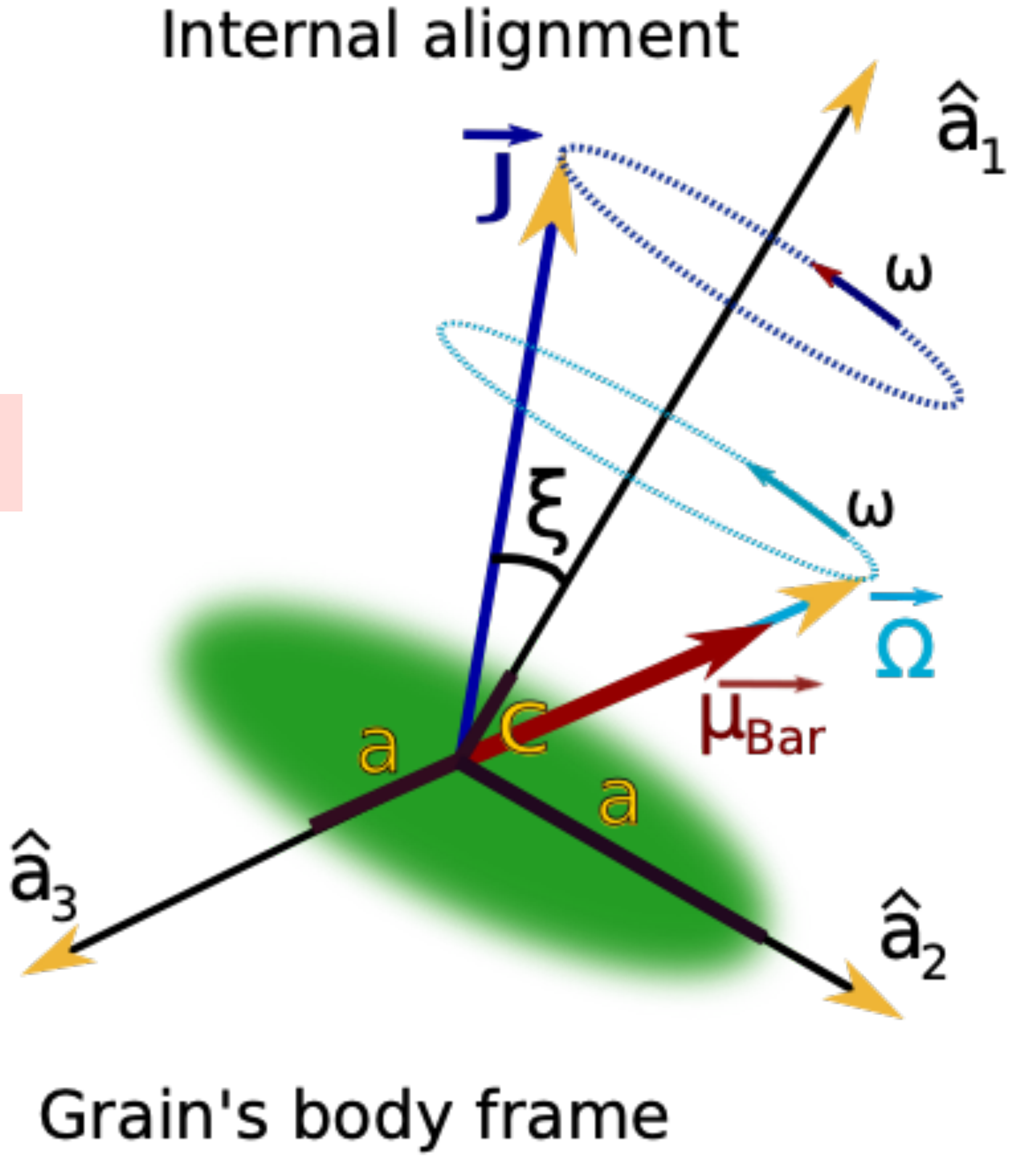

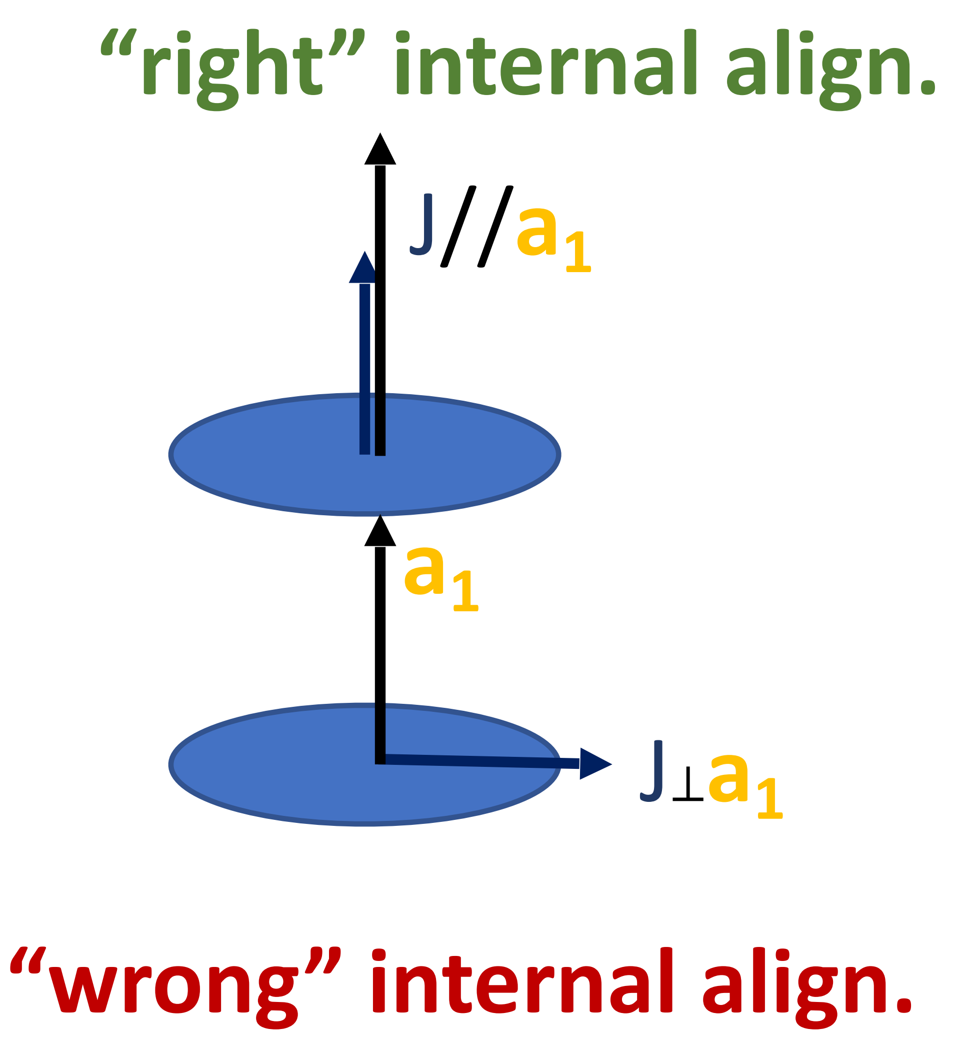

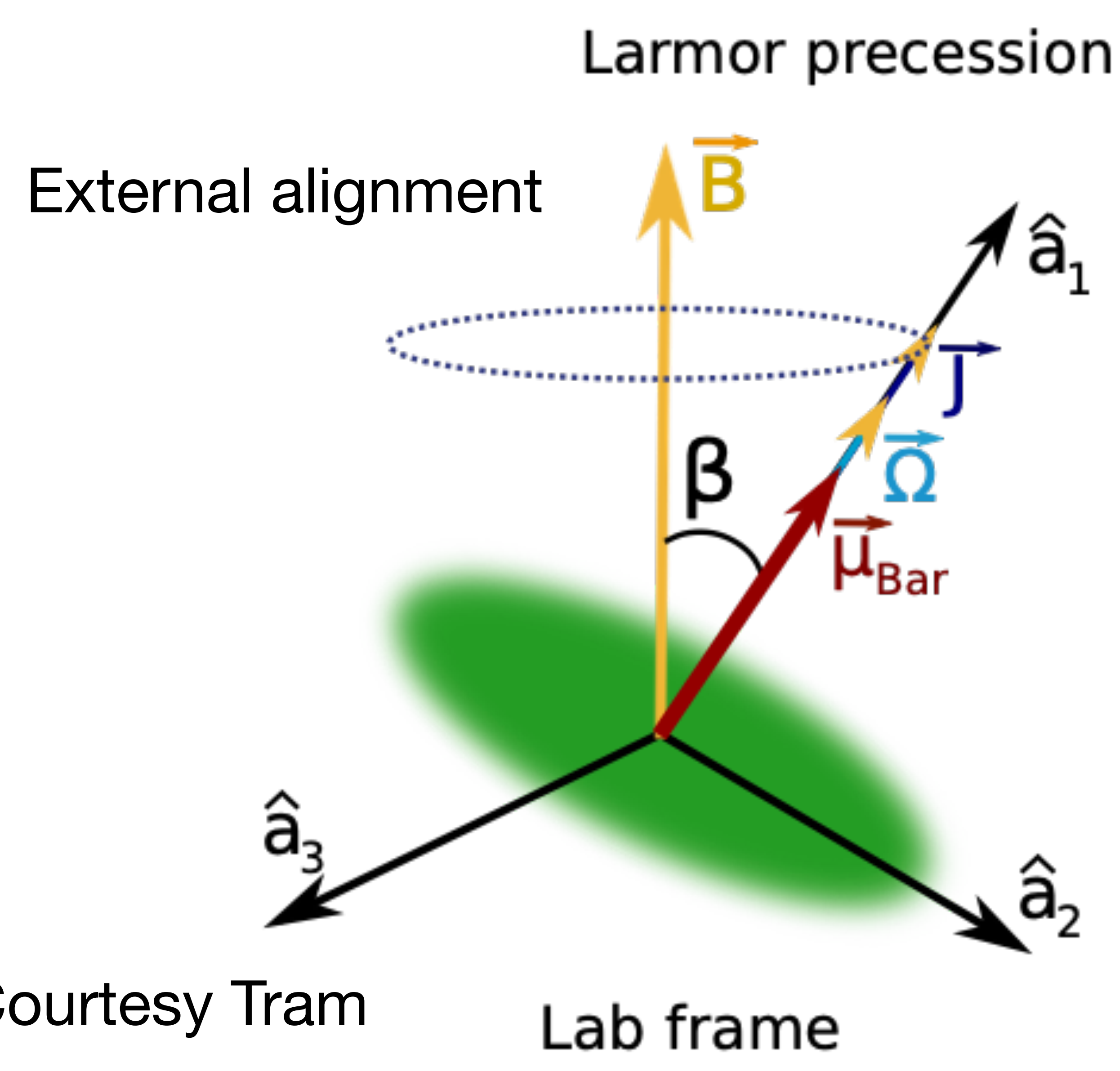

Courtesy Tram

Polarization from dust - differential absorption

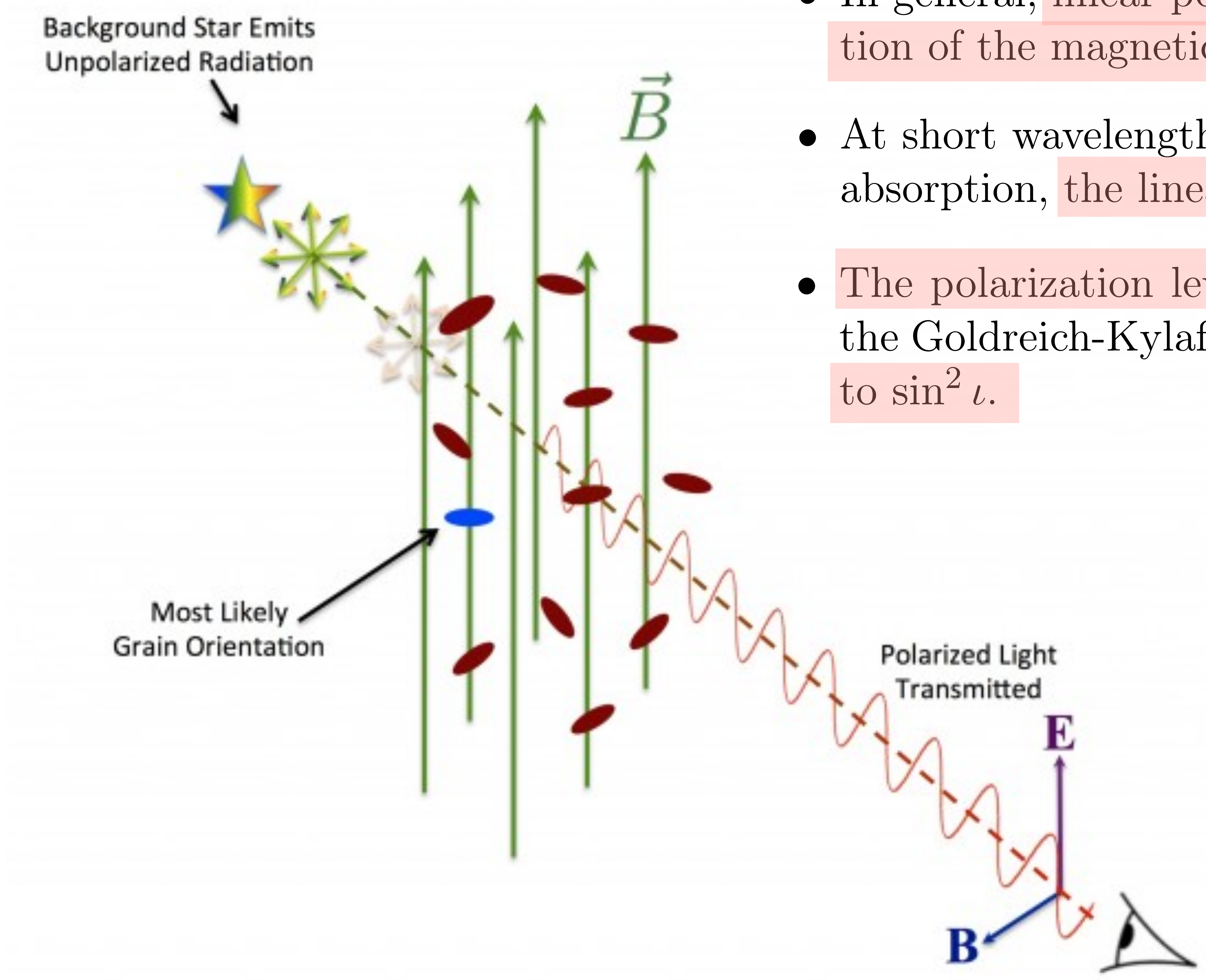

- In general, linear polarization from dust grain traces the orientation of the projection of the magnetic field on the plane of the sky.
- At short wavelengths (e.g., in the optical) where polarization is due to differential absorption, the linear polarization is aligned with the magnetic field.
- The polarization level p is independent of the magnetic field strength (similar to the Goldreich-Kylafis effect but unlike the Zeeman effect) and varies proportionally to $\sin^2 \iota$.

Polarization from dust - differential absorption

B68

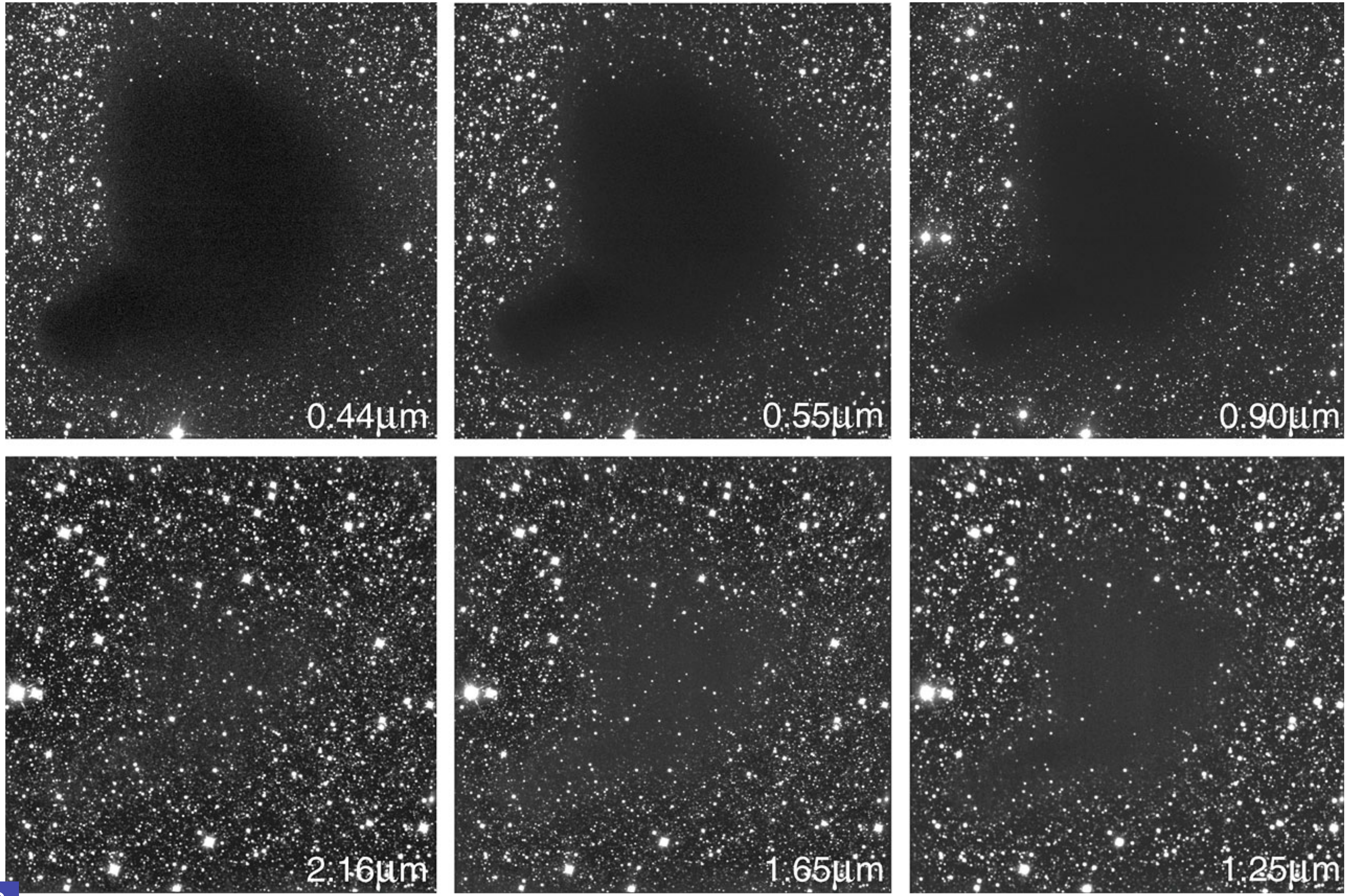

Polarization from dust - differential absorption

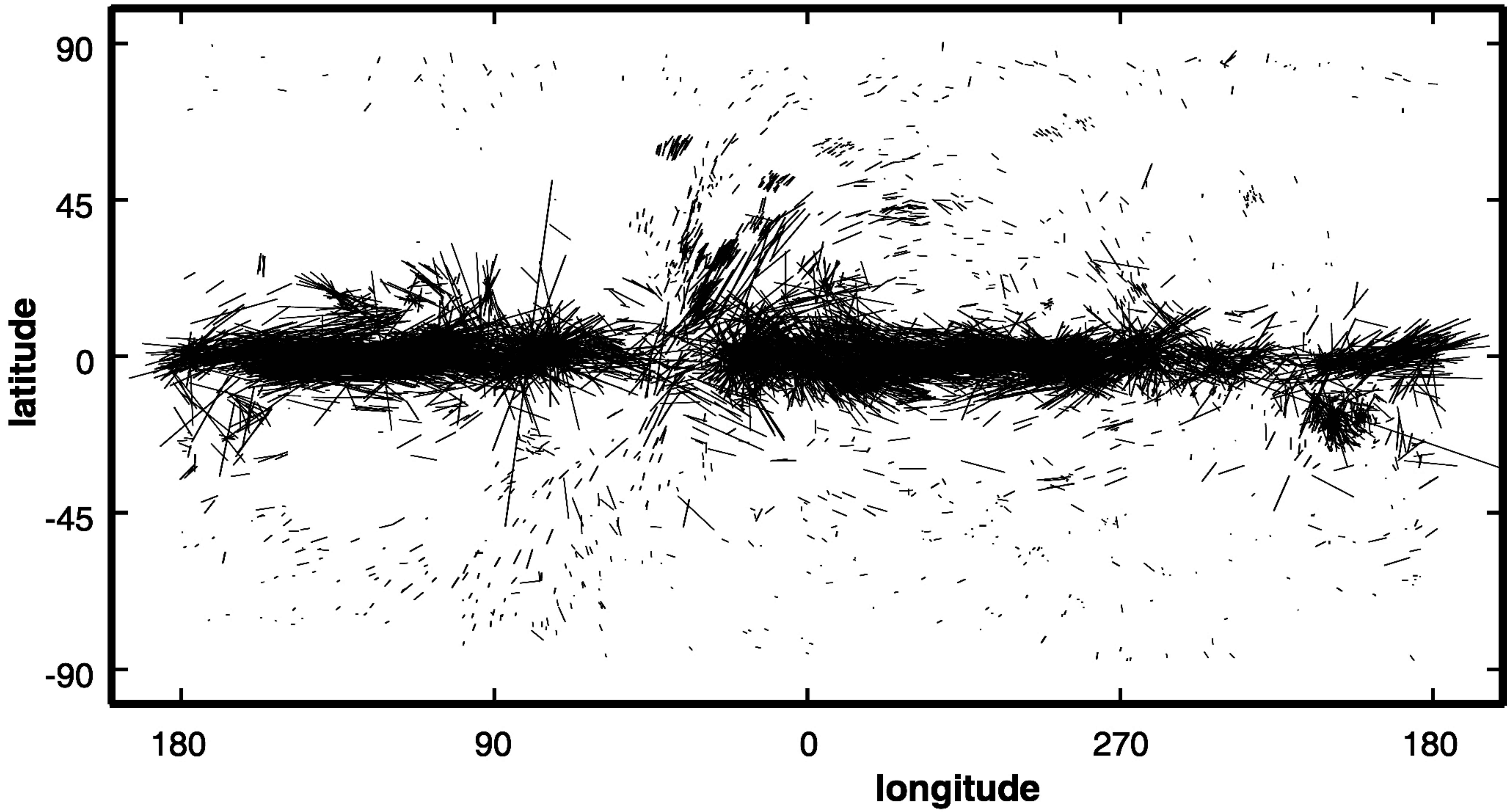

Figure 1.13: Starlight polarization measurements over the sky. At low latitudes the inferred orientation of the magnetic field follows the Galactic plane. Courtesy T. J. Jones.

Polarization from dust - emission

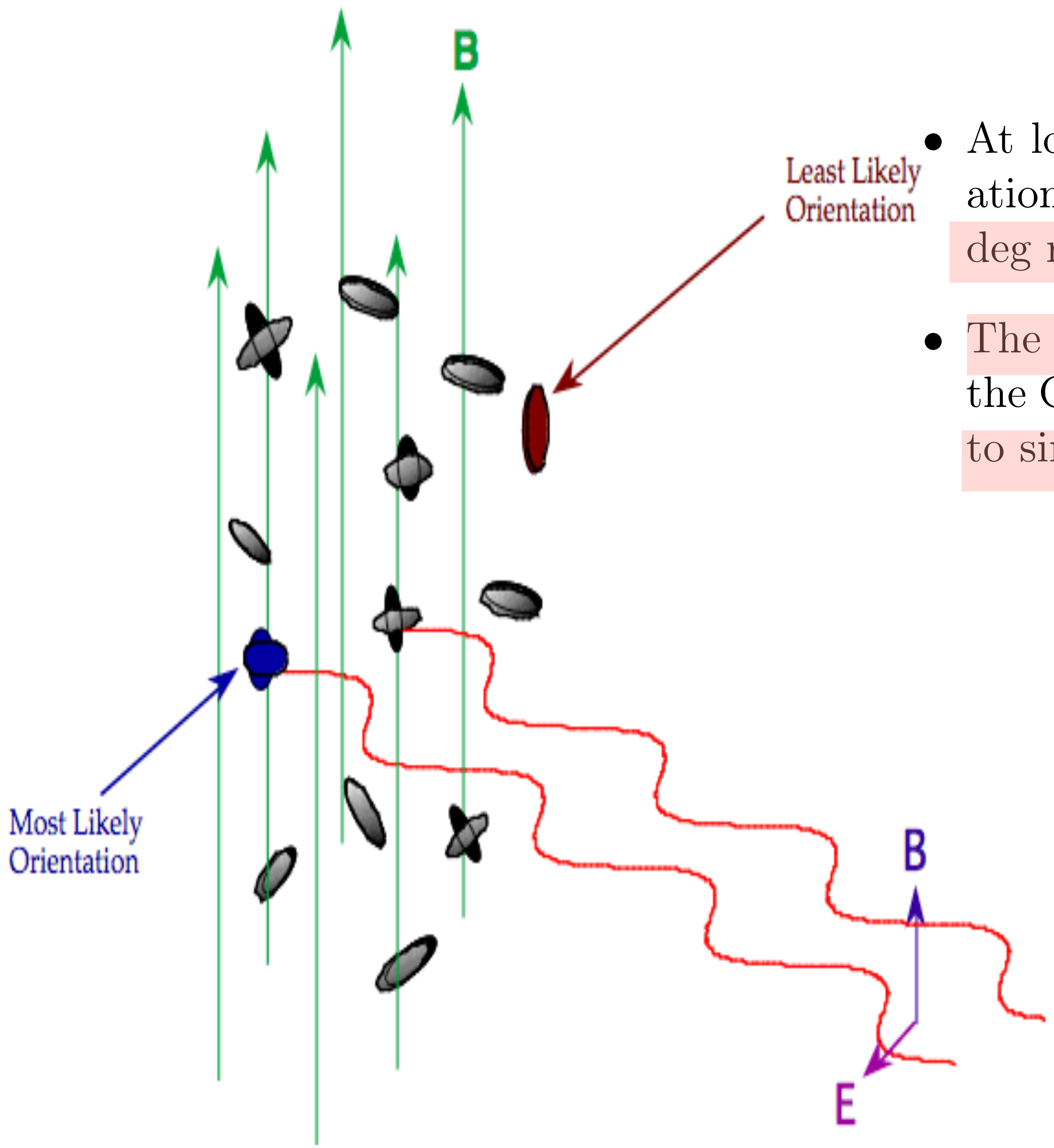

- At longer wavelengths (e.g., at FIR and mm/summ wavelengths) where the radiation emanates from the grains, the linear polarization vectors are oriented at 90 deg relative to that of the magnetic field.
- The polarization level p is independent of the magnetic field strength (similar to the Goldreich-Kylafis effect but unlike the Zeeman effect) and varies proportionally to $\sin^2 \iota$.

Polarization from dust emission + spectral line

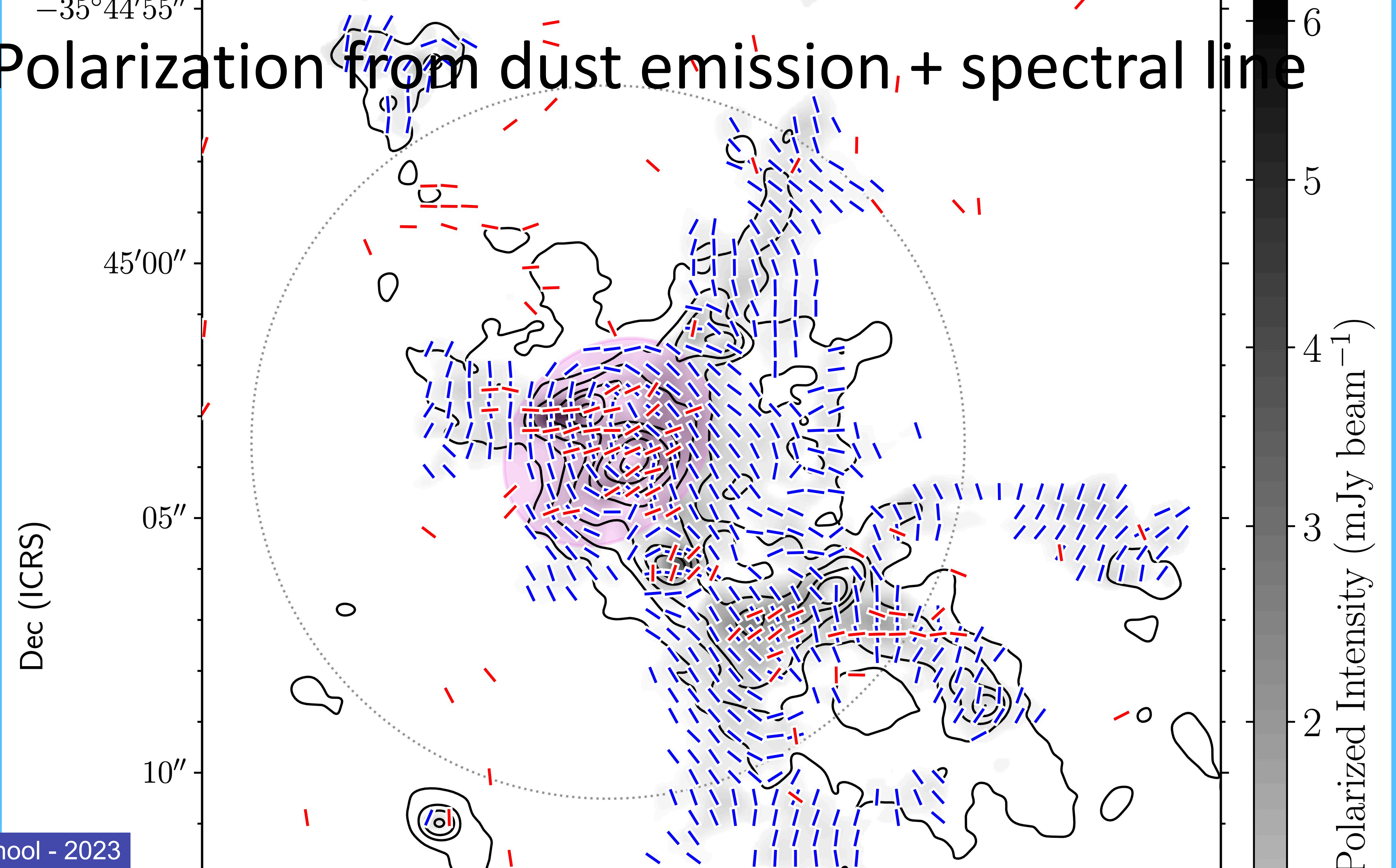

Polarization from dust - differential absorption + emission

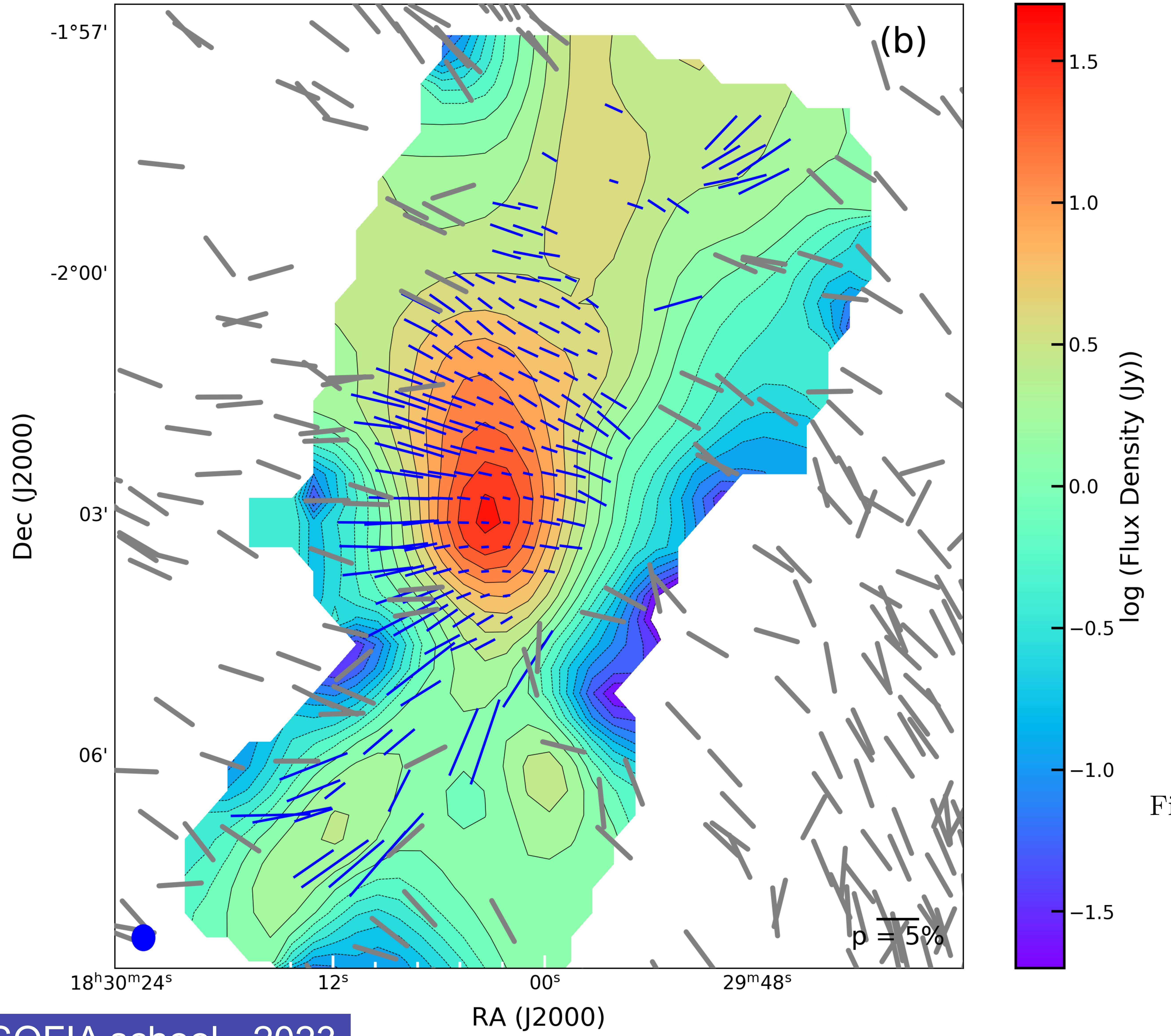

Figure 1.15: Polarimetry map of Serpens South from SOFIA/HAWC+ at 214 μm (emission; blue vectors) and with SIRPOL in the near-infrared (H band) (differential absorption; grey vectors). Both sets of vectors show the orientation of the magnetic field on the plane of the sky. From Pillai et al. 2020, Nat. Ast., 4, 1195.

Polarization from synchrotron radiation

- Radiation from acceleration — relativistic gyration about magnetic field
- For a single charge — elliptical polarization
- For a population of charges with a range of pitch angles (α)
  - relativistic beaming cancels circular polarization component

→ Polarization is linear and perpendicular to B_{pos}

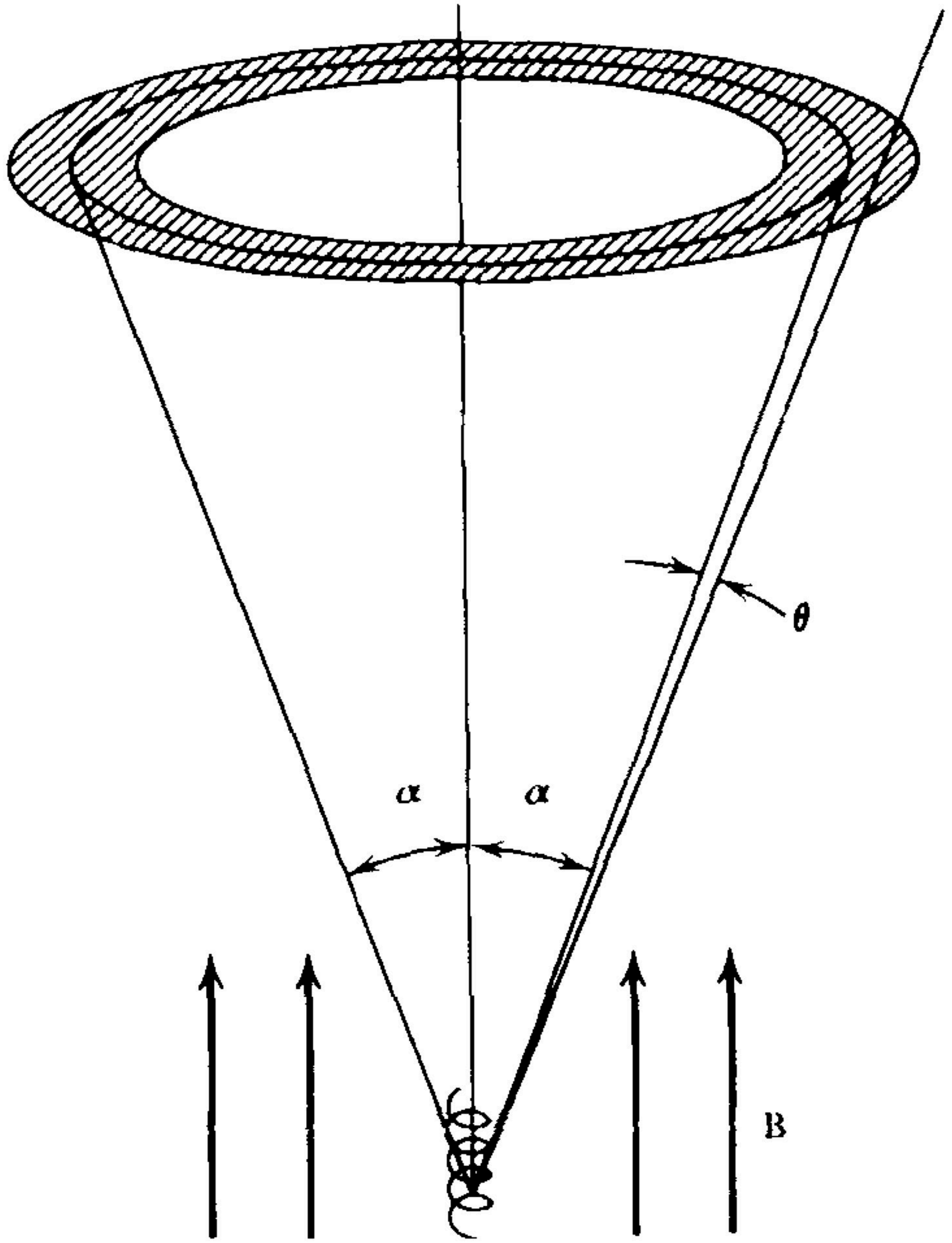

Rybicki & Lightman - Radiative processes in astrophysics, 1979 (Wiley)

Faraday rotation

- Propagation in plasma: birefringence to circular polarization modes/states

$$k_\pm = \frac{\omega}{c}\sqrt{1 - \frac{\omega_\mathrm{p}^2}{\omega(\omega \mp \omega_\mathrm{g})}}$$

with $\omega_\mathrm{p}^2 = \dfrac{4\pi q^2 n}{m}, \omega_\mathrm{g} = \dfrac{qB}{mc}$

- Rotation of linear polarization state

$$\Delta\theta(\omega) = (k_- - k_+)\frac{\Delta z}{2}$$

→ Depolarization with a dependence on frequency

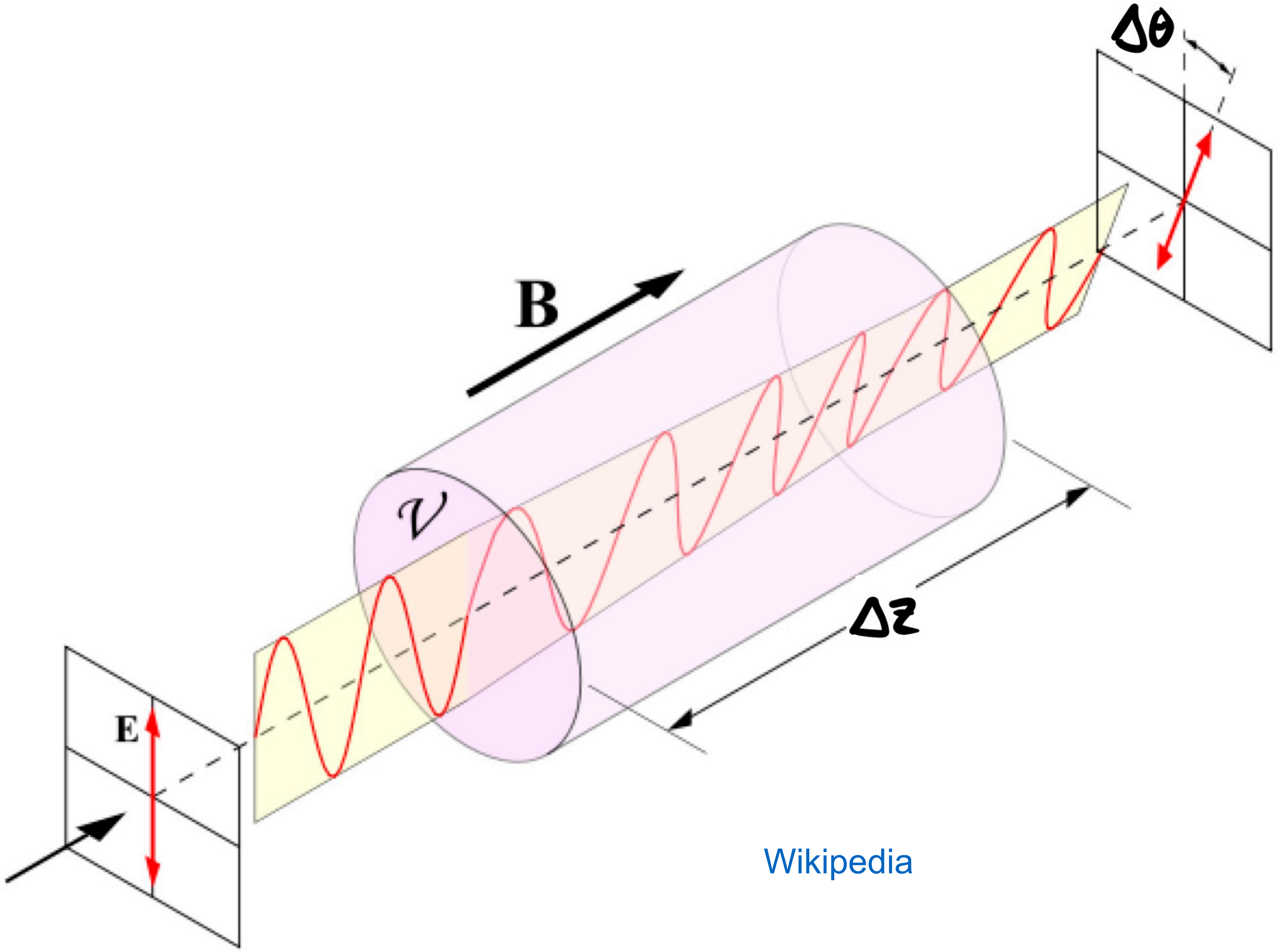

Wikipedia

Faraday rotation — magnetic field strength

- propagation time

$$\frac{dt_\mathrm{p}}{d\omega} \simeq -\frac{4\pi q^2}{mc\omega^3} \cdot \mathrm{DM}$$

with $\mathrm{DM} \equiv \int_0^{\Delta z} n dz$ → dispersion measure

- Faraday rotation

$$\frac{d(\Delta\theta)}{d\omega} = \frac{d}{d\omega}(\mathrm{RM} \cdot \lambda^2)$$

with $\mathrm{RM} \equiv \frac{q^3}{2\pi m^2 c^4} \int_0^{\Delta z} n B_\mathrm{los} dz$ → rotation measure

Faraday rotation — magnetic field strength

- propagation time

$$\frac{dt_\mathrm{p}}{d\omega} \simeq -\frac{4\pi q^2}{mc\omega^3} \cdot \mathrm{DM}$$

with $\mathrm{DM} \equiv \int_0^{\Delta z} n dz$ → dispersion measure

- Faraday rotation

$$\frac{d(\Delta\theta)}{d\omega} = \frac{d}{d\omega}(\mathrm{RM} \cdot \lambda^2)$$

with $\mathrm{RM} \equiv \frac{q^3}{2\pi m^2 c^4} \int_0^{\Delta z} n B_\mathrm{los} dz$ → rotation measure

$$\langle B_\mathrm{los} \rangle \simeq \frac{2\pi m^2 c^4}{q^3} \cdot \frac{\mathrm{RM}}{\mathrm{DM}}$$

Polarization from synchrotron radiation

M51

VLA+Effelsberg
λ3 cm & λ6 cm

B field

Fletcher+ 2011, MNRAS, 412, 2386

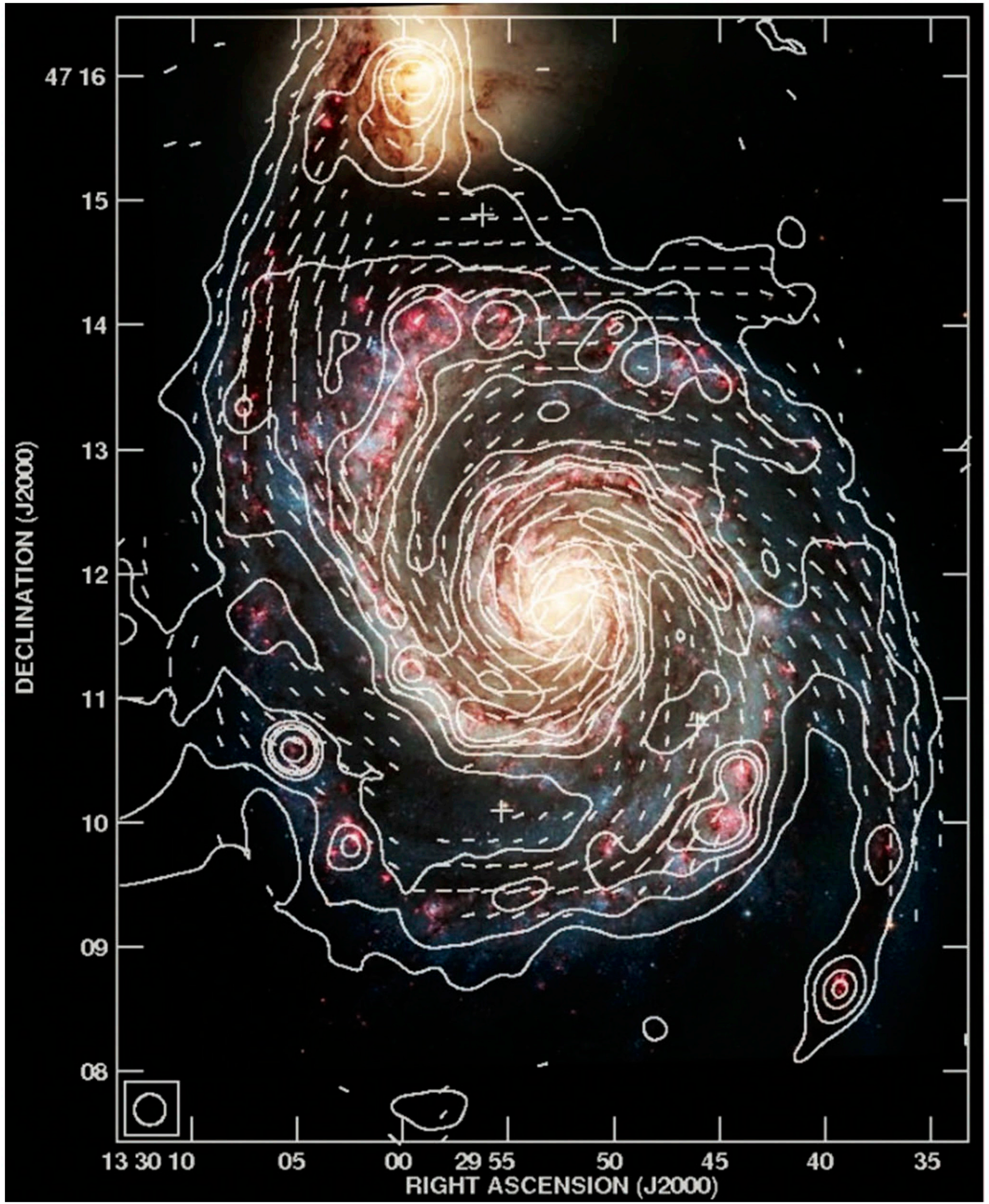

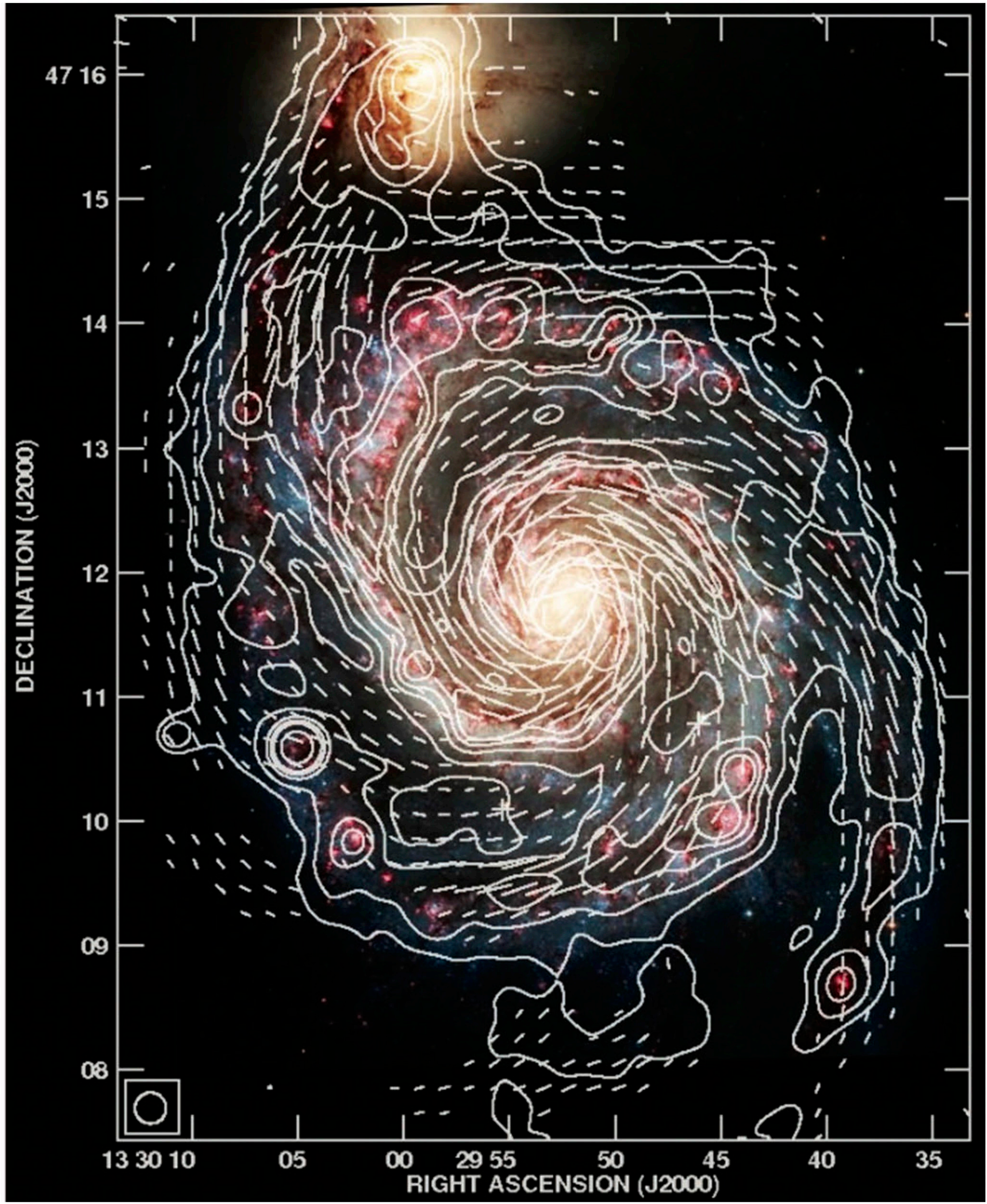

Analysis of polarization maps - DCF equation

The basic idea underlying the DCF-method consists of modelling the magnetic field with two components such that

$$\mathbf{B} = \mathbf{B}_0 + \mathbf{B}_t \tag{1.58}$$

where $\mathbf{B}_0$ and $\mathbf{B}_t$ are the large-scale (or mean or ordered) and turbulent (or random) parts of the overall field. We then assume that

- The turbulent component is weak, i.e., $B_t \ll B_0$.
- The turbulent component is zero-mean, i.e., $\langle \mathbf{B}_t \rangle = 0$.
- Deviations from the mean field are due to Alfvén waves, i.e., $\mathbf{B}_0 \cdot \mathbf{B}_t = 0$.
- And there is equipartition between turbulent kinetic and magnetic energies, i.e., $\rho v_t^2/2 = B_t^2/8\pi$.

This last equation is readily transformed to

$$v_t = \left(\frac{B_t}{B_0}\right)\left(\frac{B_0}{\sqrt{4\pi\rho}}\right), \tag{1.59}$$

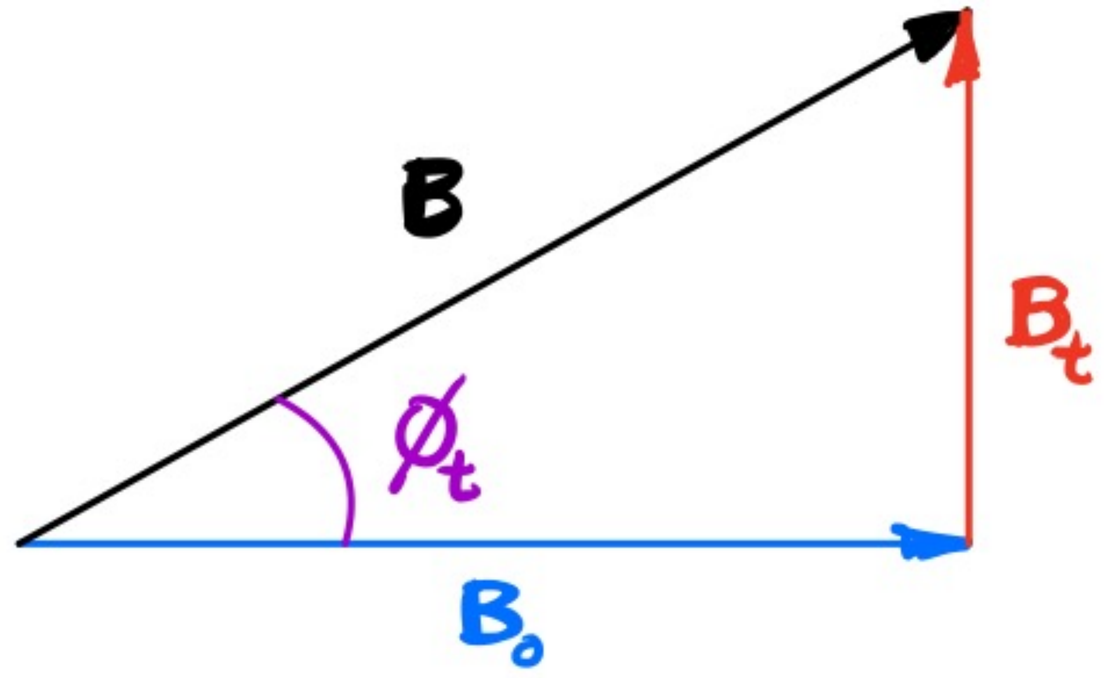

and recognizing that the polarization angle $\Delta\theta = B_t/B_0$ we arrive at the DCF equation for the plane of the sky magnetic field strength

$$B_0 = \sqrt{4\pi\rho}\frac{v_t}{\Delta\theta}. \tag{1.60}$$

Analysis of polarization maps - DCF equation

It became clear early on that the technique had several shortcomings. For example, here are a few issues

- Turbulence in the ISM is not only due to Alvén waves (compressible modes exist).
- The mean field $\mathbf{B}_0$ must be fairly close to the plane of the sky.
- The assumption of weak turbulence (i.e., $\theta \ll 1$) is often violated.
- The measured signal is integrated along the line of sight and across the telescope beam, which artificially reduces the dispersion in $\Delta\theta$ (and overestimates B_0).

Analysis of polarization maps- DCF equation

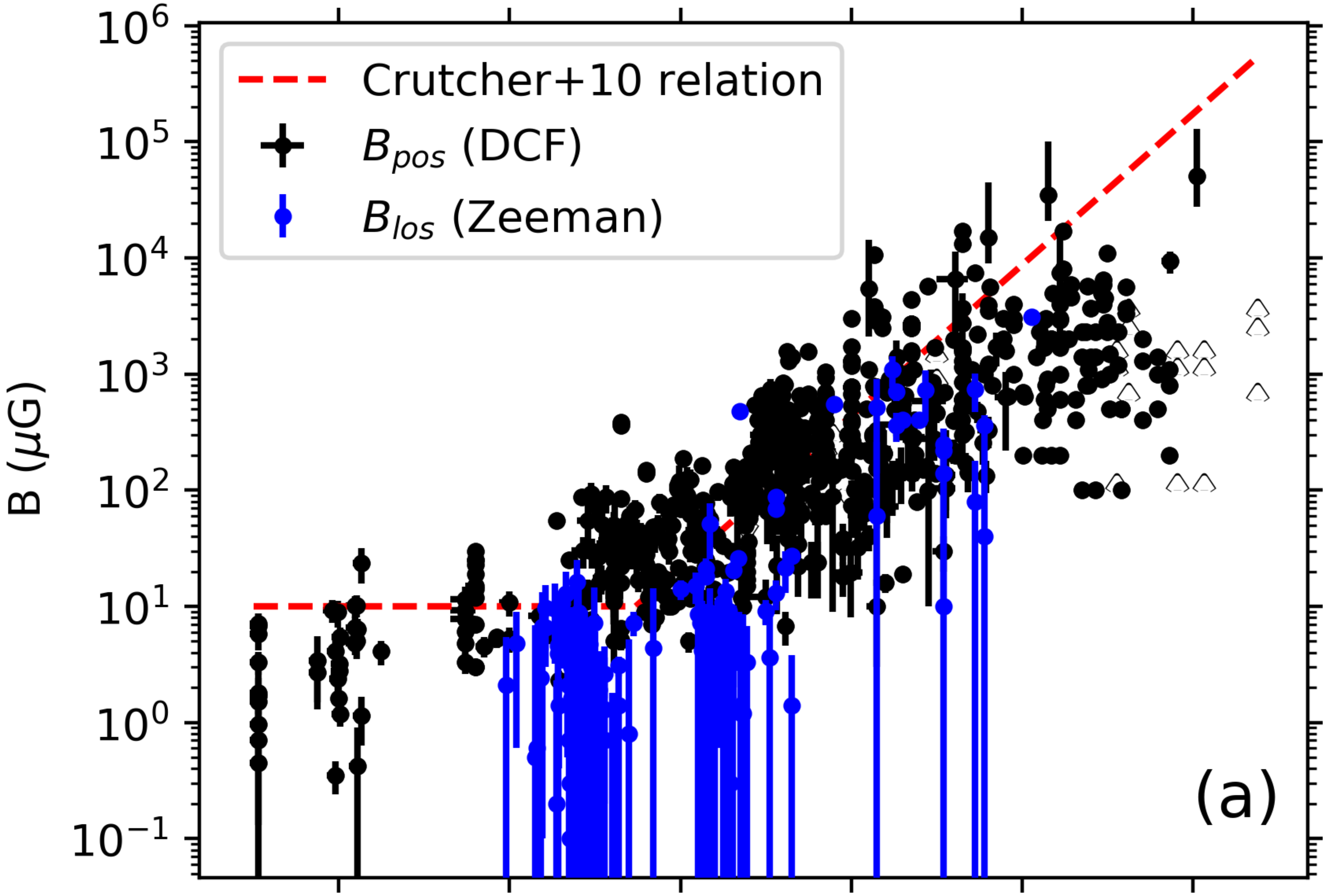

Figure 1.16: A combination of the Zeeman B_{los} measurements of Fig. 1.7 and a compilation of published estimates of the plane of the sky magnetic field strength B_0 obtained with the DCF equation. It appears that the DCF method consistently overestimates the magnetic field strength. From Pattle, Fissel & Tahani, 2022, arXiv:2203.11179v1).

Angular dispersion analysis

Improvements to the DCF method were realized when analysis techniques borrowed from turbulence studies were adopted. Namely, structure functions of the polarization angle came into play. There are several approaches and variations to this... my own preference is the following function that link changes between polarization angle at two points located a distance ℓ apart, $\Delta\theta\left(\ell\right) \equiv \theta\left(\mathbf{x}\right) - \theta\left(\mathbf{x}+\boldsymbol{\ell}\right)$, and the magnetic field at the same points

$$\begin{aligned} \cos\left[\Delta\theta\left(\ell\right)\right] &= \frac{\mathbf{B}\left(\mathbf{x}\right)\cdot\mathbf{B}\left(\mathbf{x}+\boldsymbol{\ell}\right)}{\mathbf{B}\left(\mathbf{x}\right)\cdot\mathbf{B}\left(\mathbf{x}\right)} \\ &= \frac{\mathbf{B}\cdot\mathbf{B}\left(\ell\right)}{\mathbf{B}\cdot\mathbf{B}\left(0\right)}. \end{aligned} \tag{1.61}$$

Averaging this function over a polarization map for a given separation ℓ yields

$$1 - \left\langle\cos\left[\Delta\theta\left(\ell\right)\right]\right\rangle \simeq \frac{1}{2}\left\langle\Delta\theta\left(\ell\right)^2\right\rangle, \tag{1.62}$$

which is valid for small $\Delta\theta\left(\ell\right)$ (and thus small ℓ). The function within brackets on the right-hand side of equation (1.62) is the second order structure functions of the

Angular dispersion analysis

$$1 - \langle \cos [\Delta\theta (\ell)] \rangle = \left[\frac{1}{1 + N \langle B_0^2 \rangle / \langle B_t^2 \rangle} \right] \left[1 - e^{-\ell^2/2\left(\delta^2 + 2W^2\right)} \right] + \sum_{j=1}^{\infty} a_{2j} \ell^{2j}. \quad (1.63)$$

The last term on the right-hand side is a Taylor series representation for the contribution from the large scale (or mean) magnetic field, which can be readily fitted and removed from the data, while the other term is that due to turbulence. The quantity

$$N = \frac{\left(\delta^2 + 2W^2\right) \Delta'}{\sqrt{2\pi}\delta^3} \quad (1.64)$$

is the number of turbulence cells probed by the telescope beam. Since both the turbulence correlation length δ and the effective depth Δ' of the region under study can be

Angular dispersion analysis

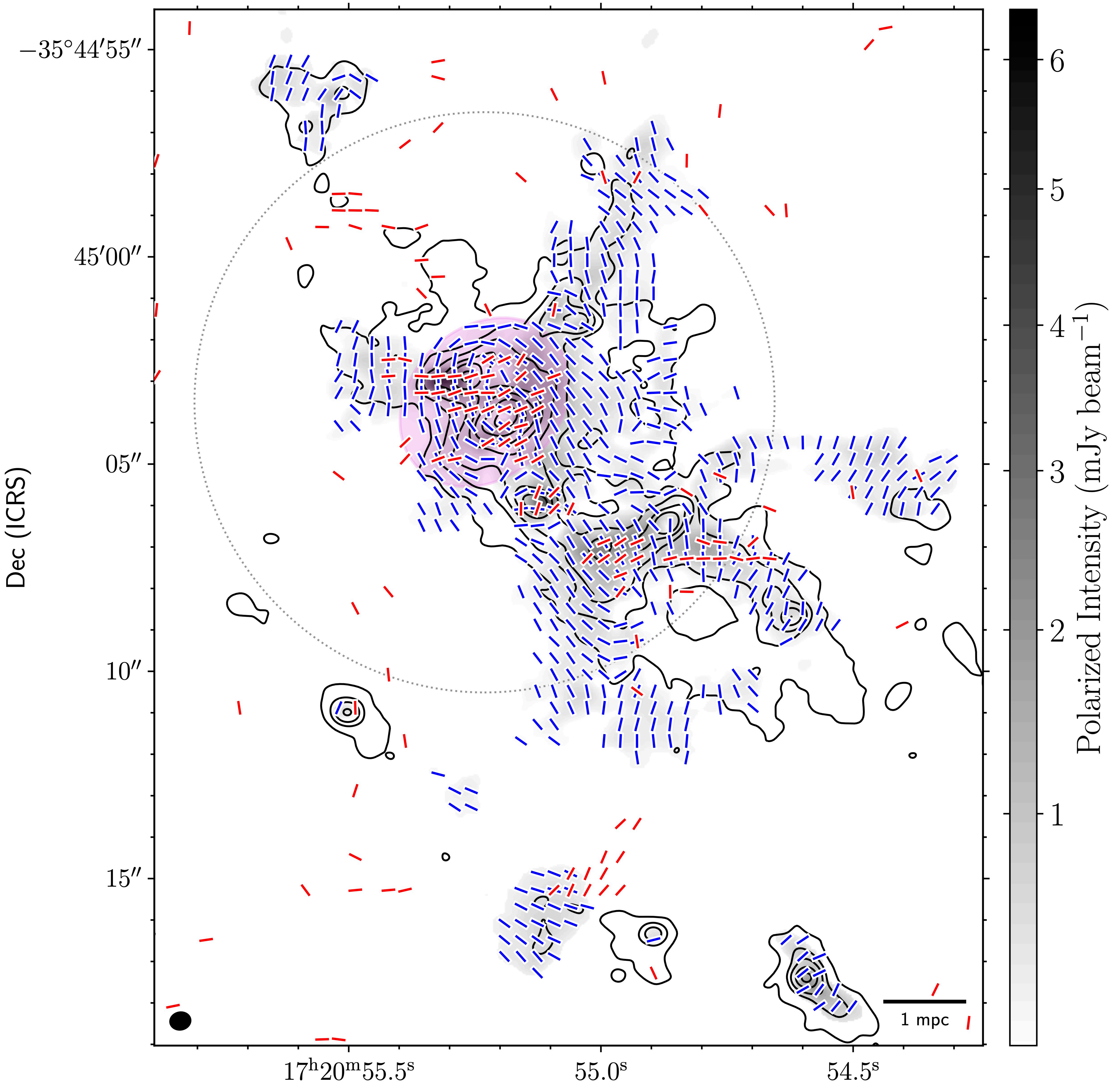

RA (ICRS)

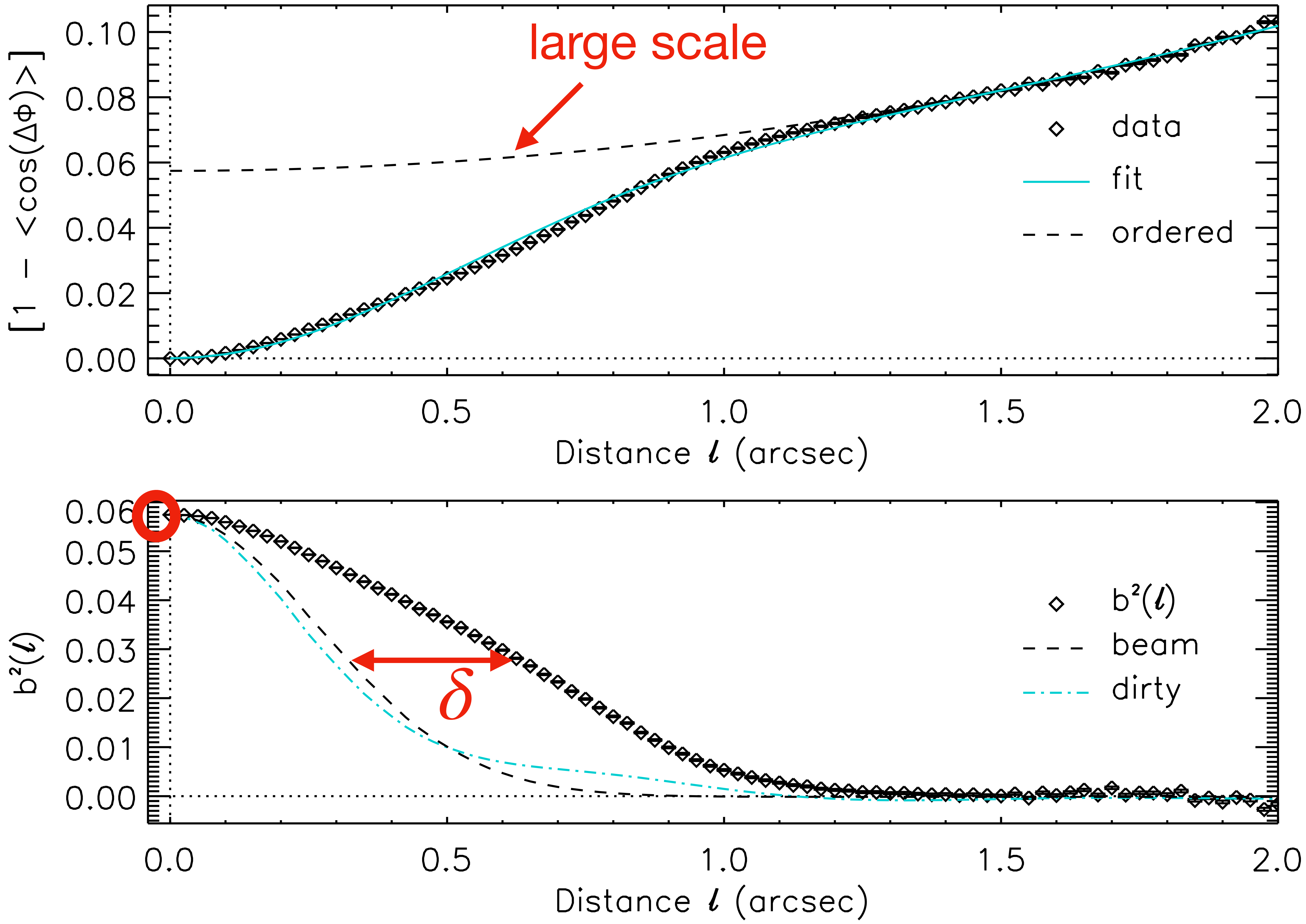

Cortés+ 2021, ApJ, 923, 204

Angular dispersion analysis

The value for the number turbulence cells found to be $N \simeq 1.4$ through equation (1.64) can be used with level at the peak of the autocorrelation function $b^2(0) \simeq 0.06$ to calculate the relative amount of turbulence in the magnetic field from

$$\begin{aligned} \frac{\langle B_t^2 \rangle}{\langle B_0^2 \rangle} &= N \left[\frac{b^2(0)}{1 - b^2(0)} \right] \\ &\equiv (\Delta\theta)^2 \,. \end{aligned} \tag{1.66}$$

The value thus calculated $\left(\langle B_t^2 \rangle / \langle B_0^2 \rangle \simeq 0.08\right)$ is then inserted in the DCF equation with an average of the spectral line width ($v_t \simeq 5.3\,\mathrm{km\,s^{-1}}$) to get a plane of the sky magnetic field strength of $B_0 \simeq 2.8$ mG.

Angular dispersion analysis - Power spectrum

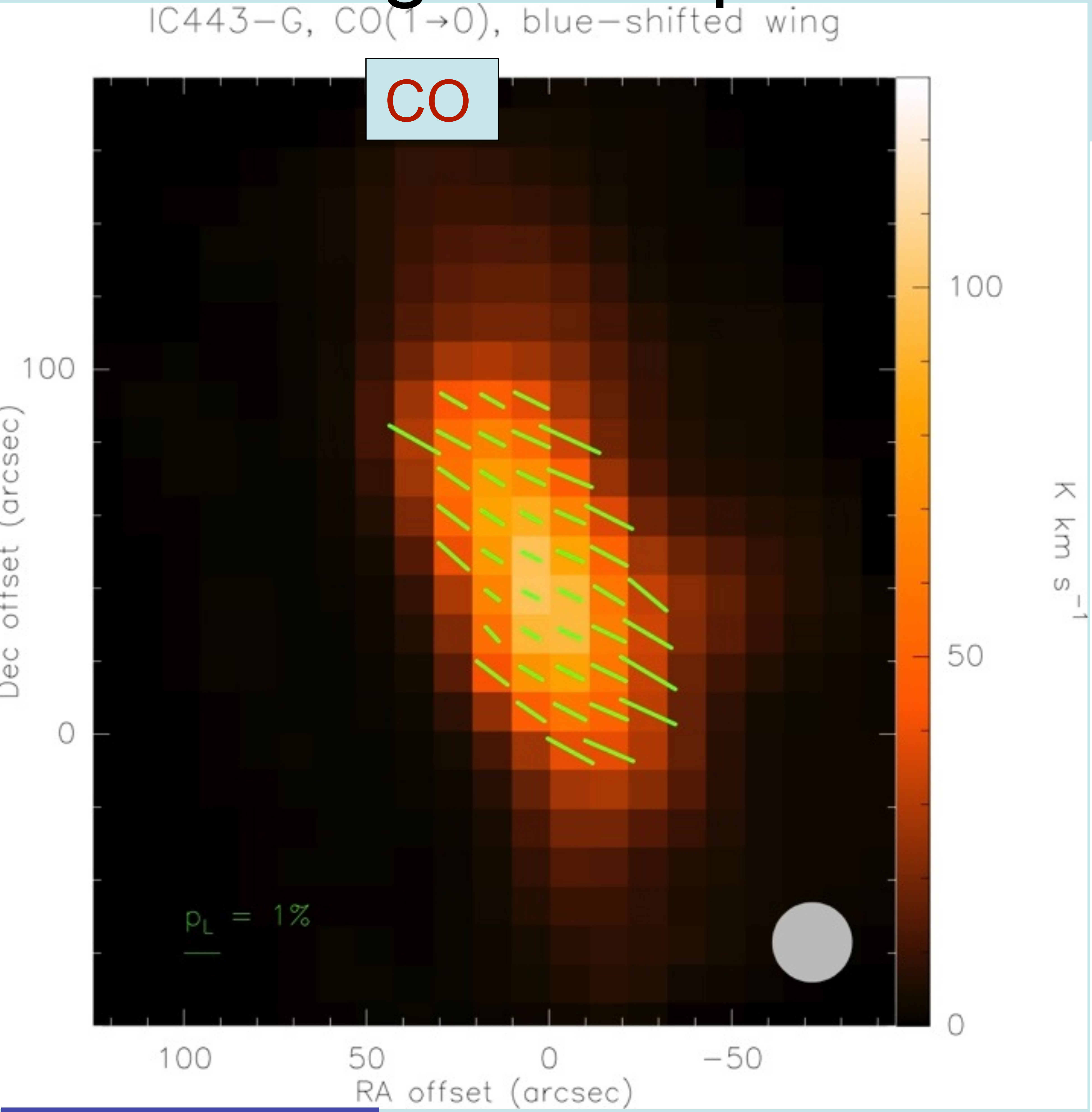

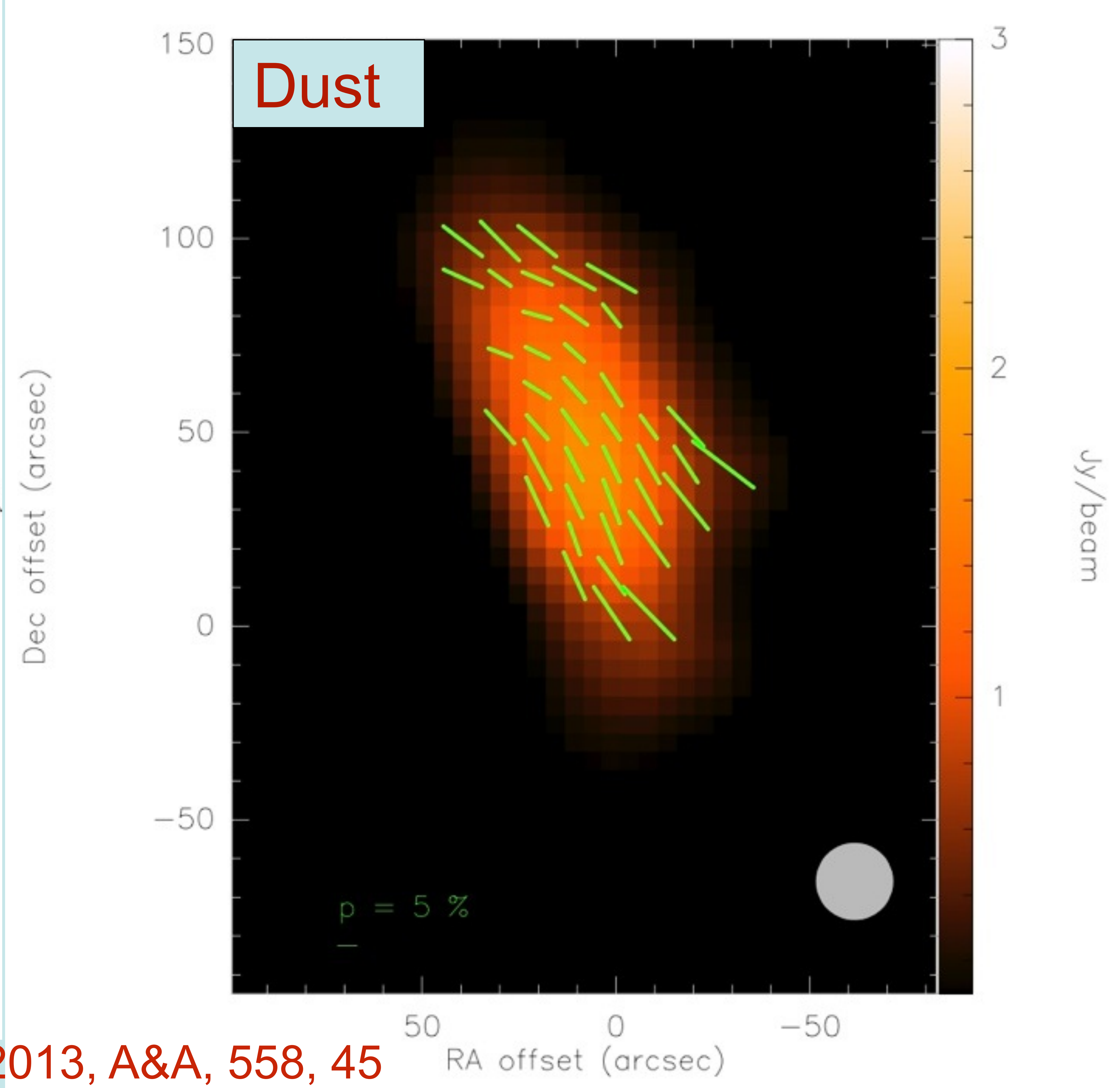

Hezareh+ 2013, A&A, 558, 45

Angular dispersion analysis - Power spectrum

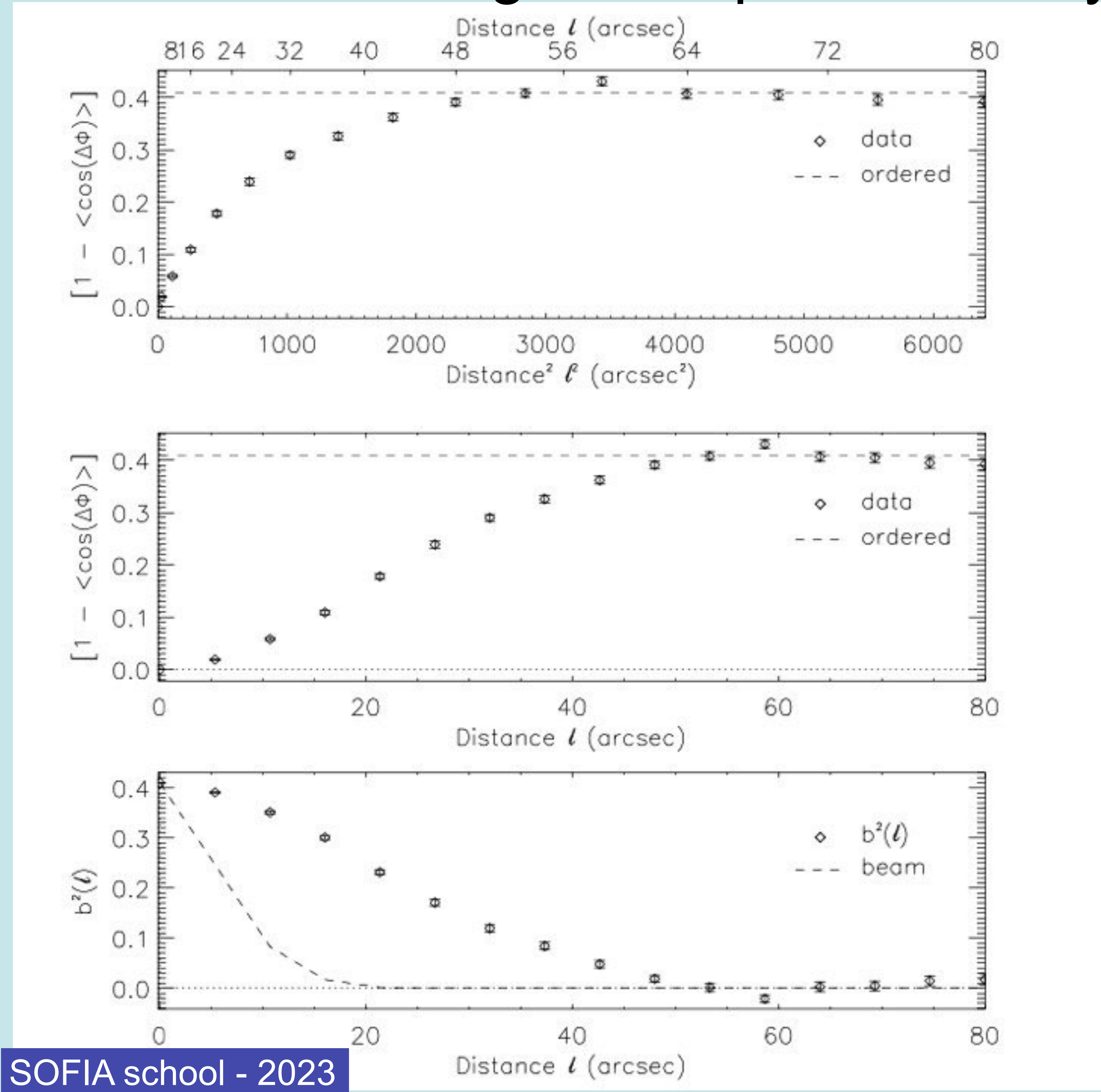

Angular dispersion analysis - Power spectrum

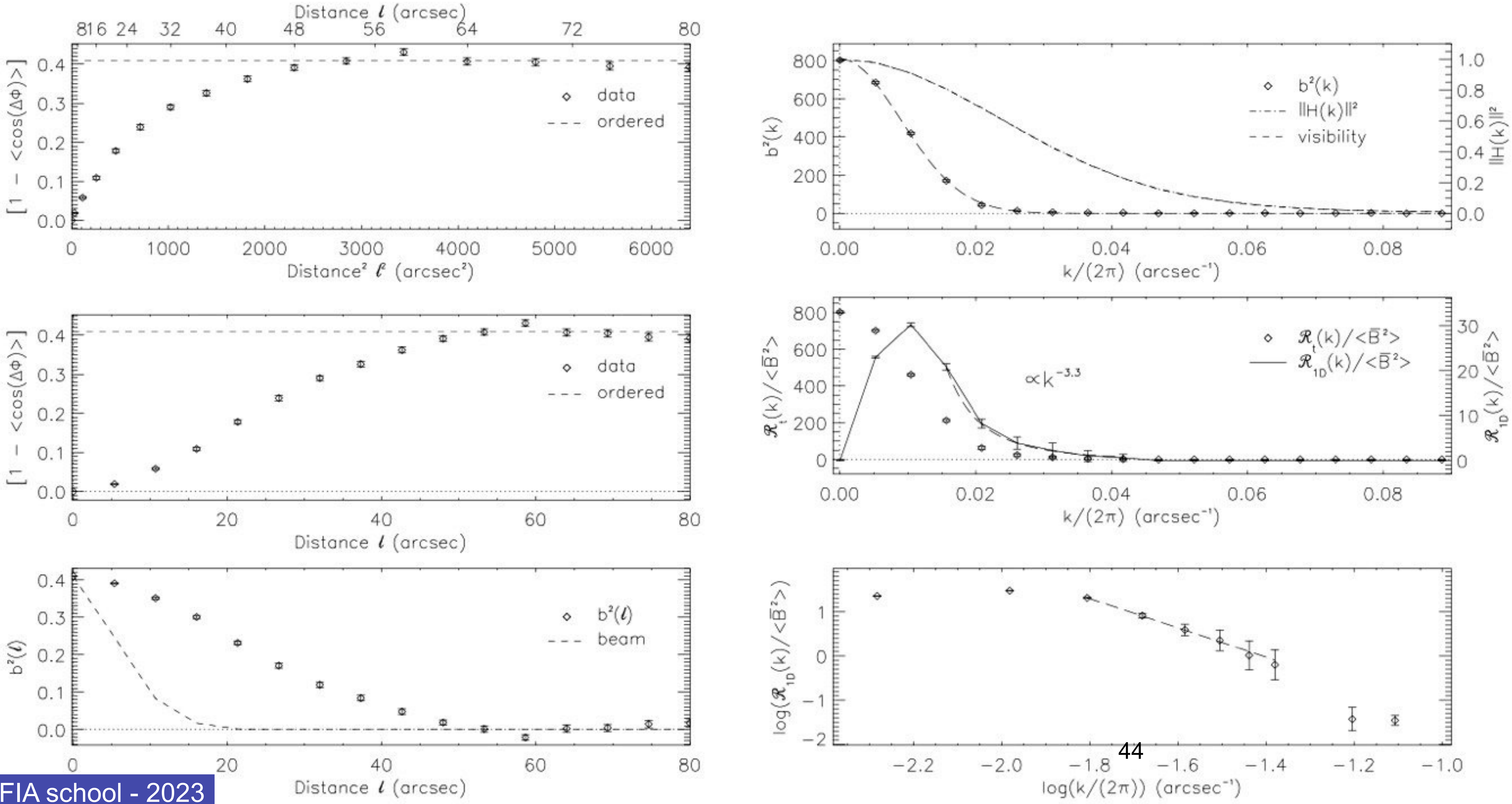

Angular dispersion analysis - Power spectrum

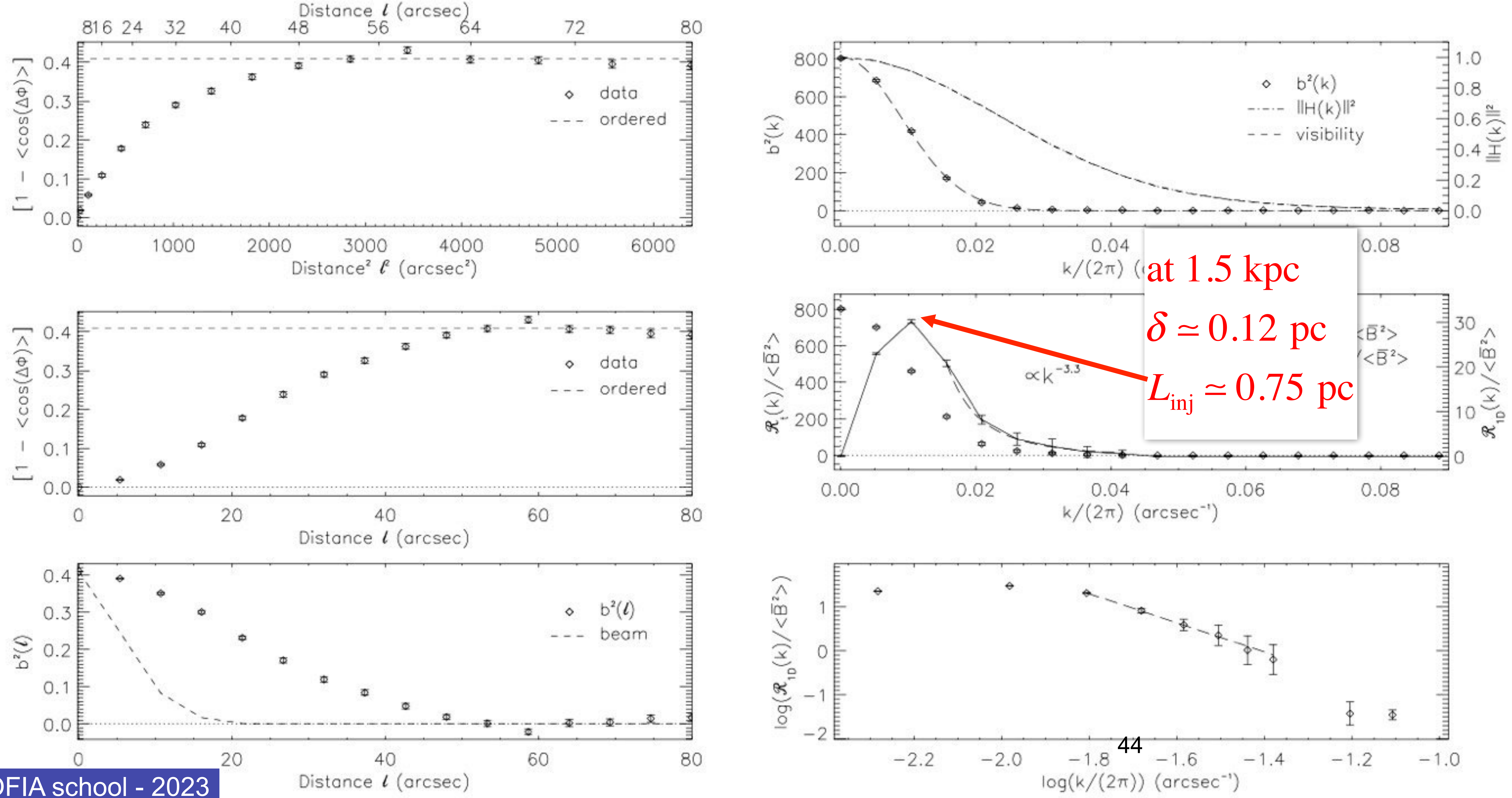

Summary

- Measuring magnetic fields is difficult...
  - Zeeman is the only direct measurement method but low SNR
    - better for masers
- Polarization from spectral lines and dust are indirect and statistical methods → imprecise with DCF
- Polarization at radio wavelengths → synchrotron and Faraday rotation
- Significant efforts to improve estimates (e.g., angular dispersion analysis)
- New techniques are being developed (Velocity Gradients Technique, Differential Measure, Anisotropic Resonant Scattering, ...)
  - Hope to go beyond DCF

Merci !

NSERC
CRSNG

Western
UNIVERSITY · CANADA